Research Square

Preprints are preliminary reports that have not undergone peer review.
They should not be considered conclusive, used to inform clinical practice,
or referenced by the media as validated information.

# Mitigating Condensate Dropout and Improving Gas Condensate Recovery through Wettability Alteration in Carbonate Rocks

**Fatemeh Kazemi**
Persian Gulf University
**Reza Azin**
reza.azin@pgu.ac.ir

Persian Gulf University
**Shahriar Osfouri**
Persian Gulf University
**Seyed Taha Hosseini**
Persian Gulf University
**Kirill M. Gerke**
Moscow Institute of Physics and Technology
**Marina V. Karsanina**
Moscow Institute of Physics and Technology
**Mohammad Sedaghat**
The University of Queensland

**Research Article**

**Keywords:** Gas condensate reservoirs, Condensate blockage, Enhanced recovery, Wettability alteration, Gas-wetting state

**Posted Date:** November 24th, 2026

**DOI:** https://doi.org/10.21203/rs.3.rs-11669860/v1

**License:** This work is licensed under a Creative Commons Attribution 4.0 International License.
Read Full License

**Additional Declarations:** No competing interests reported.

# Mitigating Condensate Dropout and Improving Gas Condensate Recovery through Wettability Alteration in Carbonate Rocks

**Fatemeh Kazemi [a], Reza Azin [b,*], Shahriar Osfouri [a], Seyed Taha Hosseini [b], Kirill M. Gerke [c], Marina V. Karsanina [c], Mohammad Sedaghat[d*]**

[a] Department of Chemical Engineering, Faculty of Petroleum, Gas, and Petrochemical Engineering, Persian Gulf University, Bushehr, Iran.

[b] Department of Petroleum Engineering, Faculty of Petroleum, Gas, and Petrochemical Engineering, Persian Gulf University, Bushehr, Iran.

[c] Center for Computational Physics, Landau School of Physics and Research, Moscow Institute of Physics and Technology, Dolgoprudny, 141701, Moscow Region, Russia

[d] Gas and Energy Transition Research Center, University of Quuensland, Australia

## Abstract

Gas condensate reservoirs, a subclass of gas reservoirs, represent an important energy resource. However, their production is often hindered by condensate accumulation in the near-wellbore region as reservoir pressure declines below the dew-point pressure, resulting in liquid blockage and lower gas recovery. In this work, to mitigate liquid blockage and improve gas mobility, an anionic fluorosurfactant combined with hydrophobic $SiO_2$ nanoparticles was used. The treatment successfully shifted the rock surface from a liquid-wetting to a gas-wetting state, as confirmed by static contact angle measurements. A

* Corresponding Author, email: reza.azin@pgu.ac.ir ; Tel: +989177730085; Fax: +987733441495.
* Corresponding Author, email: m.sedaghat@uq.edu.au Tel: +61401687786

pronounced reduction in the surface free energy of the carbonate rock was observed after treatment, with values declining from 68.64 to 1.72 mN/m. Capillary rise heights for water and condensate decreased from 24.60 mm to 4.48 mm and from 9.98 mm to 0 mm, respectively. Over time, the water contact angle decreased by 15% and the condensate by 33%, indicating better droplet stability for water. Electrical conductivity and solid% tests during core flooding showed that 5 pore volumes of the chemical solution were sufficient to induce a gas-wetting state. Spontaneous imbibition tests revealed that liquid saturations were reduced by 63.75% (water) and 33.17% (condensate) after treatment. Water permeability dropped by 72.7%, and capillary pressure increased by 23.5%. Coreflooding tests at 0.5-2 cc/min showed that increasing the flow rate decreased residual saturation from 37.54% to 11.92% and increased endpoint relative permeability from 5.17 to 9.54 mD. Following treatment, the pressure drop decreased by 38.35% for water and 21.95% for condensate, while the endpoint relative permeability increased to 1.62 and 1.28 times the corresponding pre-treatment values, respectively. These findings highlight the potential benefits of wettability modification for enhanced recovery in gas condensate reservoirs.

**Keywords:** Gas condensate reservoirs, Condensate blockage, Enhanced recovery, Wettability alteration, Gas-wetting state

## 1. Introduction

Natural gas is one of the world's most important energy resources because of its abundant reserves, high energy efficiency, favorable combustion characteristics, and lower greenhouse gas emissions than other fossil fuels, which has sustained its position as a major source of

primary energy worldwide. It is an odorless and colorless mixture of various hydrocarbons. Natural gas is predominantly composed of methane, accompanied by varying proportions of heavier hydrocarbons and non-hydrocarbon constituents, including carbon dioxide, nitrogen, and hydrogen sulfide. The exact composition depends on the geological setting and fluid evolution history of the reservoir. Natural gas is a safe and relatively environmentally friendly fossil fuel, capable of partnering with renewable energy resources. Although solar energy is widely regarded as a sustainable energy source, its intermittent availability and existing deployment constraints limit its capacity to reliably meet continuously increasing energy demands. Thus, natural gas is abundant and affordable and is an ideal partner for solar energy and other renewable energies. When natural gas is burned for energy production, fewer air pollutants and $CO_2$ are emitted than when coal or petroleum products are burned to produce the same amount of energy. Furthermore, it is a cheaper and more economical alternative to oil. All this makes natural gas one of the best non-renewable sources of energy. Natural gas reservoirs supply over a quarter of the global energy demand [1]. As shown in Figure 1, petroleum followed by natural gas, has remained the largest source of energy consumption from 1990 to the present. It is forecasted that, despite the accelerated development of renewable energy technologies, petroleum and natural gas are expected to remain the primary contributors to the global energy supply through 2050.

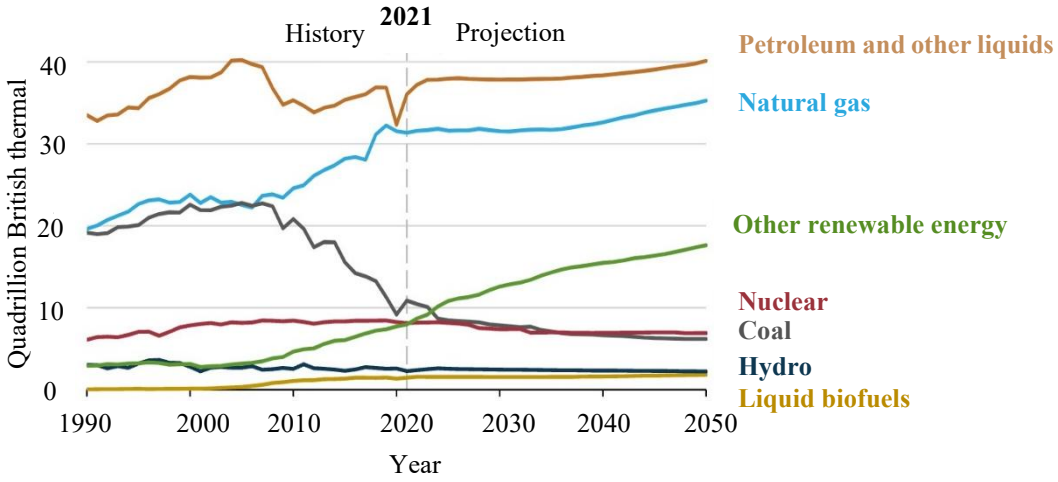



**Figure 1. World energy consumption by energy sources (1990-2040)- (Source: Energy Information Administration (EIA), Annual Energy Outlook 2022 (AEO2022)).**

Natural gas reservoirs are conventionally classified into three main types based on their phase behavior and fluid composition: dry gas, wet gas, and gas condensate reservoirs [2]. Retrograde condensation is initiated in gas condensate reservoirs as reservoir pressure decreases below the dew-point pressure. Gas condensate reservoirs contain a significant fraction of the world's natural gas reserves, making them an important source of hydrocarbon production [3]. In addition to natural gas, these reservoirs produce valuable condensate liquids with considerable commercial significance. Consequently, improving condensate recovery has become a major research priority because of its direct impact on the economic performance of gas condensate reservoirs. Gas condensate reservoirs are commonly associated with reservoir pressures of 3,000–8,000 psi and temperatures between 200 and 400 °F [4]. Nevertheless, depending on fluid composition and reservoir conditions, gas condensate systems can also occur at pressures below 2,000 psi and temperatures lower than

100 °F. These reservoir fluids are composed primarily of methane and other light hydrocarbons, together with a limited amount of heavier hydrocarbon fractions that condense when reservoir pressure falls below the dew-point pressure. In the region away from the wellbore of a gas condensate reservoir, in which the pressure of the reservoir is above the dew point and the temperature of the reservoir is between the critical and cricondentherm temperatures, the only present and flowing phase is the gas phase [5, 6]. During the production life, when the reservoir pressure drops below the dew point at reservoir temperature (between critical and cricondentherm), the intermediate or heavy hydrocarbon components in the gas phase begin to condensate and liquid drops out while the liquid phase is immobile owing to the existence of capillary forces and low liquid saturation [5, 6]. Liquid drops occur first near the wellbore region and then propagate radially away along with the pressure drop. By more pressure decrement near the wellbore region, condensate saturation may be increased to a higher value of critical saturation that could flow, and condensate blockage may accrue [6-8]. The saturation of condensate near the wellbore can reach significant levels, ranging from 40% to 70% [9, 10]. The fate of this condensate can be twofold: it may either flow with the produced gas stream or become trapped within the reservoir pore space due to capillary forces [11]. The distinctive flow behavior of gas condensate systems arises from the complex distribution of condensate within the pore structure and the relatively low interfacial tension between the gas and condensate phases. Consequently, applying concepts developed for conventional gas–oil systems directly to gas condensate reservoirs may result in inaccurate interpretations of their flow characteristics.

Gas production is decreased by a factor of three to five because of liquids-condensate and water-blockage [12, 13]. Condensate accumulation around the wellbore in gas condensate

reservoirs is a complex phenomenon influenced by a multitude of factors. Fluid properties like phase behavior and interfacial forces, rock properties such as wettability, and flow regime (Darcy vs. non-Darcy) all play a role. External forces like gravity also contribute [14]. Understanding the interplay between fluid dynamics and interfacial interactions near the wellbore is crucial for optimizing gas and condensate flow. Research in this area is ongoing, as the industry seeks to fully grasp the impact of these factors. The dominant forces governing flow within the reservoir are capillary, gravitational, and viscous. In the bulk reservoir, low velocity allows gravity and capillary forces to dominate. However, near the wellbore, the balance between viscous and capillary forces becomes critical [15]. Since manipulating viscous forces is often impractical, reducing interfacial forces is a promising approach to improve recovery by increasing the capillary number [16]. Above the dew point, where the gas remains a single phase, factors like reservoir permeability, thickness, and gas viscosity dictate production efficiency. However, below the dew point, the scenario changes dramatically. Here, the key determinants of wellbore productivity shift to critical condensate saturation and the relative permeability of both the gas and condensate phases. This underlines the importance of understanding how reservoir fluid behavior changes with pressure for optimal well performance.

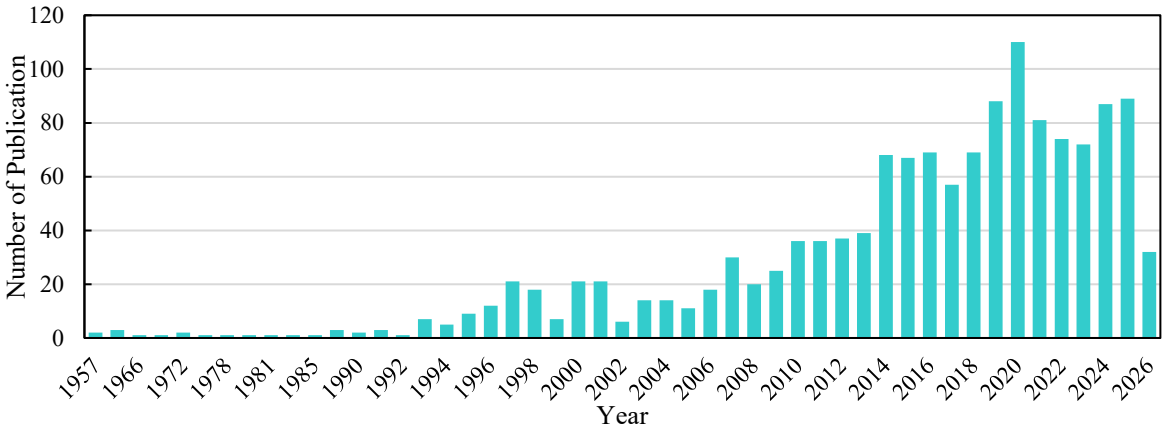
Many fields in the world face this problem. Therefore, any possibility to study this kind of reservoir and production improvement of gas and condensate is highly appealing. It is important to note that condensate has been found to have several applications in industry and daily life [17]. The heavy part of the gas is more precious compared to the gas phase, specifically in areas away from the gas market and transportation systems [12].

Furthermore, the presence of formation water leads to water blockage around the wellbore and, in general, unsuitable conditions - well deliverability drops [18]. Liquid water introduces the third phase to the reservoir besides the gas and gas condensate phases, by which the multiphase flow conditions may further decrease the effective permeability of the gas phase. Altogether, the hydrocarbon production may degrade further [19-23]. The water blockage also happens in the bulk of the reservoir, especially in tight gas reservoirs that have smaller grains and, thus, pore throats that lead to higher capillary pressure and higher irreducible water saturations, and so affect the effective permeability of the gas phase [24]. In the gas reservoir, if the water sources are huge and the water permeability is high, the water invades the gas zone, leading to a large amount of gas being trapped with a significant decrease in its recovery factor [25, 26]. Therefore, finding an appropriate strategy to overcome liquid blockage (condensate and water) around the wellbore and improve the gas and condensate production is essential.

Bibliometric analysis was conducted to provide an overview of the current research status, trends, and leading developments in gas condensate reservoir studies. This aims to serve as a reference for researchers undertaking follow-up studies in this area. For this purpose, performance analysis was carried out using the Web of Science (WoS) database, and the bibliometric mapping was executed using VOSviewer software. VOSviewer (VOS is an abbreviation for Visualization of Similarities) is a software tool for constructing, visualizing, and exploring bibliometric maps of science [27].

“Gas condensate reservoir” OR “condensate gas reservoir” OR “gas condensate” OR "retrograde gas condensate reservoir*" OR "Condensate banking" OR "Retrograde condensation" OR "Near-wellbore condensate dropout" OR "Condensate blockage" AND

144 “reservoir*” were used a the search query in the WOS core database, with 1394 publications
145 until July 2026 is published on the subject of gas condensate reservoirs. Figure 2 presents the
146 annual publication trend of gas condensate reservoir research indexed in the WoS database.
147 The earliest publication on this topic was recorded in 1957, whereas research output remained
148 limited throughout the following decades. From 1997 onward, research activity accelerated,
149 leading to continuous growth in the annual number of publications, which reached nearly 110
150 by 2020. Figure 3, illustrates the varying degrees of research activity across different
151 countries, emphasizing that China, USA, Russia, Canada, and Iran have substantial
152 contributions to the study of condensate gas reservoirs.



153

**Figure 2. Annual trends of publications in the gas condensate reservoir subject from 1957 to 2026.**

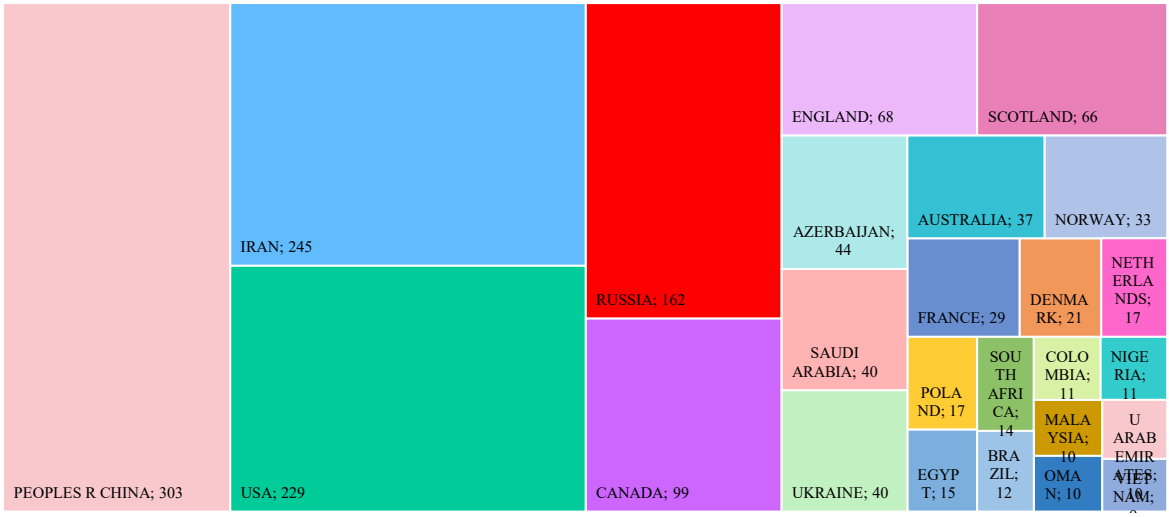



**Figure 3. Countries with high study contributions in the field of gas condensate reservoirs.**

Moreover, Figure 4 provides insights into the activity and number of publications of 25 top researchers, highlighting the scope of their engagement and influence in advancing knowledge within this specific field. The varying sizes of the rectangles, each representing a researcher, may indicate the frequency of their contributions, offering a detailed perspective on the research scene.

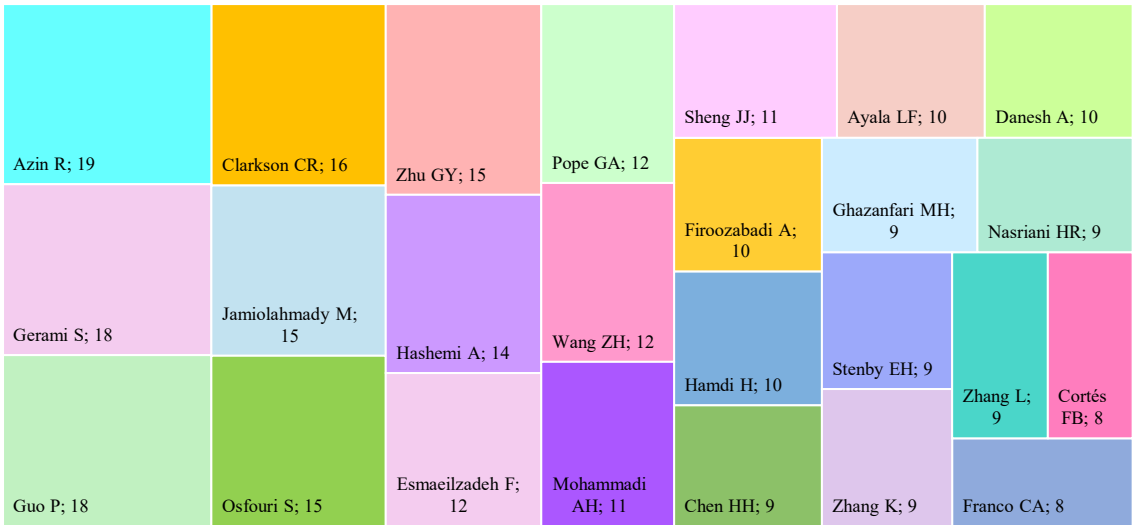



**Figure 4. Researchers with high study contributions in the field of gas condensate reservoirs.**

Then, other keywords, "wettability alter*" OR "gas wet*" OR "liquid repel*" were added to the previous search in WOS. The result was 97 documents, which were the input data for the VOSviewer software. The text-mining module of VOSviewer enables the construction of term co-occurrence networks based on information extracted from publication titles, abstracts, or author-assigned keywords. [28]. VOSviewer is specifically designed to work with documents written in English. A term map is a two-dimensional representation where terms are positioned in a manner that signifies the relatedness of the terms through the distance between them. Typically, a smaller distance indicates a stronger connection between two terms. The determination of term relatedness is based on their co-occurrence in documents (titles, abstracts, or full texts).

To improve the reliability of the co-occurrence network, only author keywords with more than two occurrences in the WoS core database were included in the analysis. Accordingly, 25 out of the 208 identified keywords satisfied the selection criterion and were used for

network construction. Figure 5 presents the co-occurrence analysis of author keywords associated with wettability alteration in gas condensate reservoirs. Wettability alteration was the most influential keyword, exhibiting the highest occurrence (33) and the greatest total link strength (TLS) (76), indicating its central role in the research network. Gas condensate reservoirs (26 occurrences; TLS = 53), Gas-wetting ranked third, with 23 occurrences and a TLS of 61, highlighting its close association with wettability modification studies, and condensate blockage (15 occurrences; TLS = 39) also occupied prominent positions, reflecting the strong emphasis on condensate banking and production impairment in this research area. Keywords including surface free energy, contact angle, nanoparticles, wettability, and fluorosurfactant (FS) exhibited moderate (10-4 occurrences; TLS = 29-12), demonstrating their importance in characterizing and achieving wettability alteration.

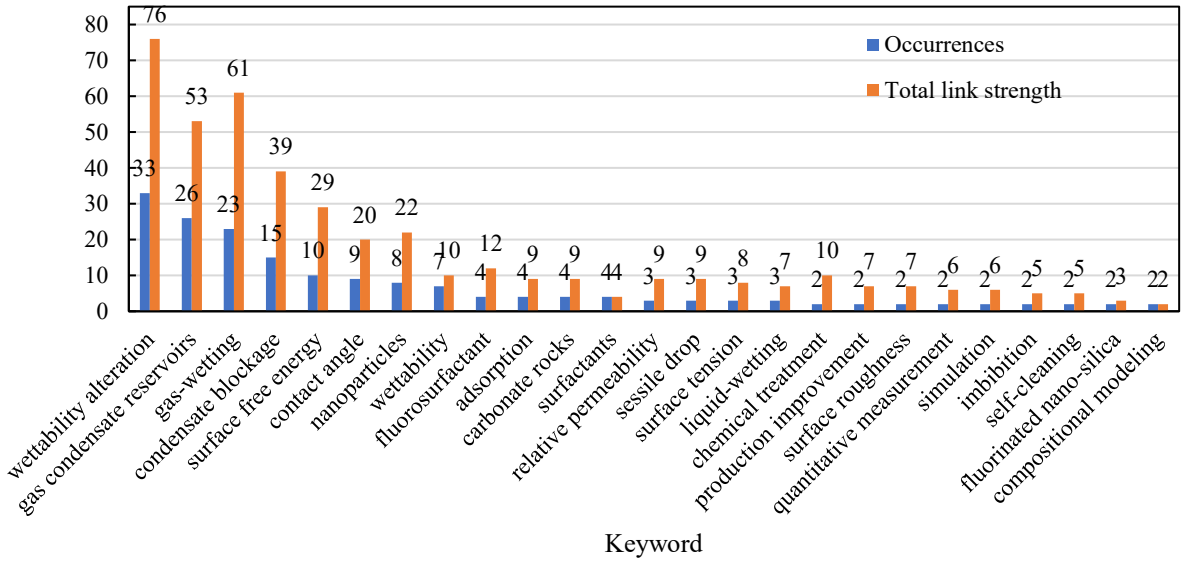



**Figure 5. Co-occurrence map of author keywords related to wettability alteration in gas condensate reservoirs.**

VOSviewer supports the visualization of bibliometric networks through three distinct representations: network, overlay, and density visualizations. The visualization includes the 25 author keywords with more than two occurrences in the WoS Core Collection. Each node represents an individual keyword, and its size is proportional to the number of occurrences. Links connecting the nodes denote keyword co-occurrence within the same publication, whereas a shorter distance between two nodes indicates a stronger association between them. Also, a lighter color of the line indicates a minimal connection between the words. Keywords such as “wettability alteration”, “gas condensate reservoirs” and “gas-wetting” occurred most commonly, indicating that these three keywords constitute the primary focus of the existing literature, and “compositional modeling” was the least frequently used keyword. Figure 6, presents the overlay visualization of keyword co-occurrence generated by VOSviewer. In this visualization, keywords are colored according to their average publication year, where purple indicates earlier studies and yellow represents more recent topics. The results show that “surface tension”, “optimization”, “compositional modeling”, and “surface roughness” are among the most recently emerging keywords, highlighting current research interests and

emerging trends in wettability alteration for gas condensate reservoirs.

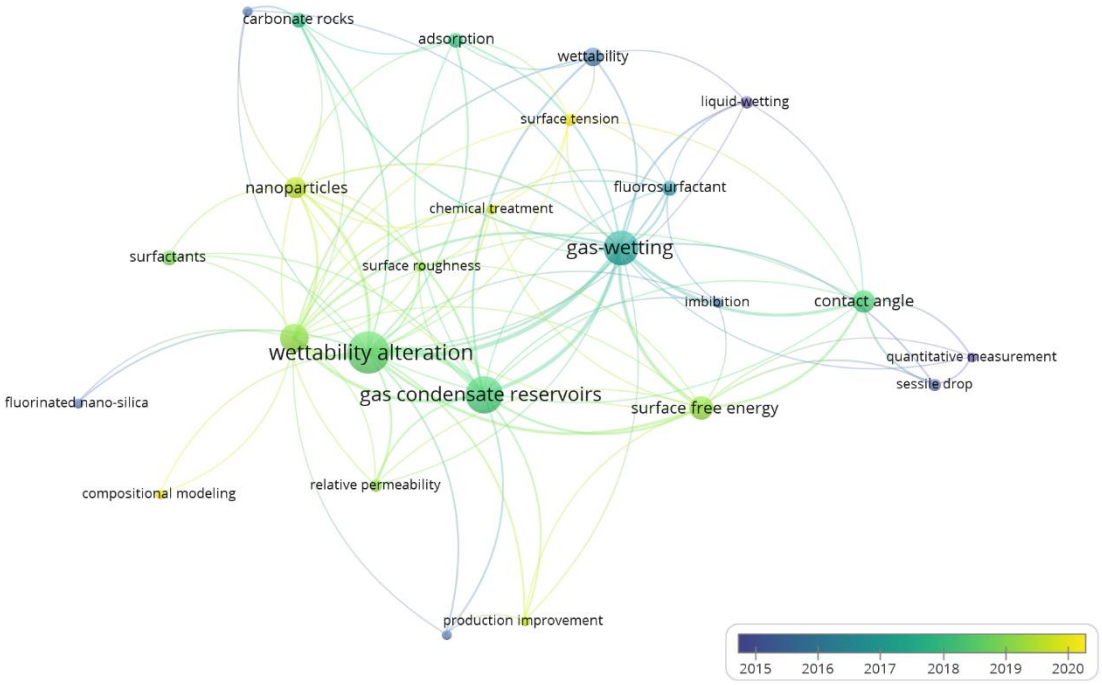
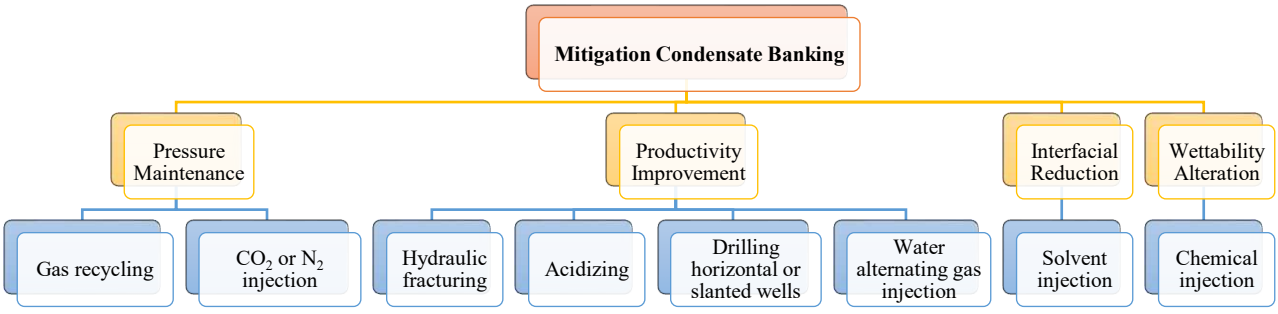



**Figure 6. Overlay visualization of keywords co-occurrence**

Maximizing gas recovery from condensate reservoirs is critical to meet future energy demands. There are different solution techniques to increase the reservoir pressure and alleviate the condensate dropout, including gas recycling, hydraulic fracturing, acidizing,



drilling horizontal or slanted wells, water alternating gas injection (WAG), solvent injection, and chemical injection Figure 7 [29].

**Figure 7. Condensate-banking mitigation strategies [8].**

These methods are currently used in industry, and each of them has different applicability depending on the formation and the regulations of the region. Among various enhanced gas recovery (EGR) techniques, chemical treatment agent injection, whose most important mechanism is wettability alteration, plays a vital role in reducing residual condensate saturation and improving well production permanently [30]. Therefore, wettability alteration may offer a more durable solution for enhancing recovery from gas condensate reservoirs than most existing techniques, whose effectiveness is often temporary because condensate can reform and re-establish condensate blockage [31]. The first study of wettability alteration on a gas condensate reservoir was performed by Li and Firoozabadi [31]. The use of wettability alteration chemicals, such as FS and fluoropolymers, can present an effective solution to the condensate- and water-banking phenomena in gas condensate reservoirs. The rock mineralogy and the properties of formation water, as well as the selection of the solvent and the fluorinated chemical, are among the parameters that greatly affect the performance of the wettability alteration process. Several parameters, such as the cost of the treatment, its effectiveness and durability, the flexibility of the design to accommodate varying reservoir conditions, and the short payout time, may encourage the use of the wettability alteration method over the other techniques to mitigate the problem of condensate banking. Moreover, because the treatment is confined to the near-wellbore zone, wettability alteration offers a practical and economically attractive method for improving well performance [32].

The efficiency of wettability modifiers depends on reservoir conditions and rock–fluid properties [33-35]. Among the available materials, fluorinated compounds are particularly attractive because they effectively reduce surface free energy (SFE), thereby improving liquid repellency [31, 34, 36, 37]. Table 1, provides an overview of previous studies investigating chemical agents for wettability alteration in gas condensate reservoirs. A series of experimental techniques, including contact angle measurements, capillary rise, spontaneous imbibition (SI), entry capillary pressure determination, and coreflooding, were employed to evaluate the ability of the proposed chemicals to alter the wettability of different rock types toward gas-wet conditions.

**Table 1. Summary of previous studies on chemically induced wettability alteration in gas condensate reservoirs.**

| Chemical | Base fluid | Porous media | Tests for wettability alteration | Ref. |
|---|---|---|---|---|
| FC754 cationic surfactant, FC722 Polymer with MW 100,000 | Water-based | Berea sandstone and chalk<br>Porosity: 20.5-29 %<br>Permeability:1.47-1,089 mD | • Contact angle<br>• Capillary rise test<br>• Spontaneous imbibition<br>• Entry capillary pressure<br>• Coreflooding | [31] |
| Fluorochemical polymers FC-759 and FC-722 from 3M Company | Water-based | Berea sandstone and chalk<br>Porosity: 20-32%<br>Permeability:1.3 -500 mD | • Coreflooding | [38] |

| | | | | |
|---|---|---|---|---|
| Fluorochemical polymers FC-759 and FC-722 from 3M Company | Water-based | Berea sandstone and chalk<br>Porosity: 20% and 31%<br>Permeability:320 mD and 1.3 mD | • Spontaneous imbibition<br>• Coreflooding | [39] |
| Different surfactants | Ethanol<br>Water<br>Water/ethanol<br>Fluorinated solvent | Limestone | • Contact angle<br>• Imbibition tests | [40] |
| Fluorochemical Surfactant 11-12P, Fluoroacrylate Copolymer L-19062 from 3M Company | Ethanol, water, acetic acid | Sandstone | • Contact angle<br>• Spontaneous imbibition | [41] |
| Fluorinated surfactant | Methanol<br>Blend of methanol and water | Berea sandstone | • Contact angles<br>• Imbibition tests<br>• Core flooding | [42] |
| 30 wt% fluoropolymer in water | Water-based | Sandstone<br>Porosity: 10-20%<br>Permeability: 0.2-5.0 mD | • Contact angles<br>• Imbibition tests<br>• Core flooding | [34] |
| Nonionic polymeric fluorinated surfactant, Novec FC4430 from 3M Company | Glycol-alcohol | Sandstone | • USBM wettability index | [43] |
| Fluorochemicals | Isopropyl alcohol,<br>Brine | Limestone | • Contact angle<br>• Spontaneous imbibition | [44] |
| Fluorocarbon surfactant (WA12) | - | gas-condensate reservoir (Donpu reservoir) | • Contact angle<br>• Spontaneous imbibition<br>• Coreflooding | [45] |

| | | | | |
|---|---|---|---|---|
| Synthesize Zirconium oxide ($ZrO_2$) nano-fluids | Water-based | Carbonate | • Contact angle<br>• Imbibition tests | [46] |
| Anionic commercial surfactant Silnyl®FSJ (SY) | Water | Sandstone | • Contact angles<br>• Coreflooding<br>• Spontaneous imbibition | [47] |
| | Water/Organic Solvents | Glass Networks Pore diameter:0.2922 mm Throat diameter: 0.2 mm | • Contact angle<br>• Gas-wetness measurement for microscopic models | [48] |
| Fluoroalkyl silane functionalized $SiO_2$ nanoparticles | Ethanol | Limestone Porosity:28.4% Average pore diameter: 4.3 μm Permeability:1.5-2.0 mD | • Contact angle<br>• Coreflooding | [49] |
| Polymeric surfactant | Ethanol | Limestone Porosity:25% Permeability:3-3.5 mD | • Contact angle<br>• Imbibition tests | [50] |
| Anionic and non-anionic FSs | Methanol | Carbonate, limestone and dolomite | • Contact angle<br>• Core flooding | [51] |
| Fluorochemical polymers Zonyl8740 from DuPont Company | Water-based | Sandstone | • Contact angle<br>• Capillary rise test<br>• Spontaneous imbibition | [52] |
| Anionic and nonionic FSs | Water/ethanol | Carbonate Porosity:20.8-29.5 % | • Contact angle<br>• Core flooding | [53] |

| | | | | |
|---|---|---|---|---|
| | | Permeability:10- 122 mD | | |
| Anionic fluoro-surfactant | Water/ethanol | Carbonate<br>Average porosity:28.3 % | • Contact angle<br>• Imbibition test | [54] |
| Fluorohexyltriethoxy silane-$SiO_2$ nanocomposite | IPA and ethanol<br>Water and methanol | Limestone<br>Porosity:27%<br>Average pore diameter: 8μm<br>Permeability: 2-2.5 mD | • Contact angle<br>• Core flooding | [55] |
| Superhydrophobic $TiO_2$, $SiO_2$ and CNT | Fluorochemicals in an alcoholic medium | Carbonate | • Contact angle and<br>• Spontaneous imbibition tests | [56] |
| Silicon-based molecules and fluoro-polymer in commercial SurfaPore M nanofluid. | Water-based with very low volatile organic compounds in commercial *SurfaPore M* nanofluid | Carbonate<br>Porosity: 20%<br>Permeability: 30 mD<br>Sandstone<br>Porosity: 24%<br>Permeability: 190 mD | • Contact angle and<br>• Spontaneous imbibition<br>• Core flooding | [57] |
| FG40, FP-2, and FG40 modified nano-silica | Water-based | Sandstone | • Contact angle,<br>• Owens two liquid method<br>• Glass capillary tube rise test<br>• Imbibition tests | [58] |
| Fluorosilane | Isopropyl alcohol | Carbonate and sandstone | • Contact angle | [59] |

| | | | | |
|---|---|---|---|---|
| Fluorinated silica nanoparticle | Butanol | Sandstone | • Contact angle measurement<br>• Coreflooding | [60] |
| Gases:<br>R143A (1,1,1-trifluoroethane),<br>R125 (1,1,1,2,2-pentafluoroethane)<br>R134A (1,1,1,2-tetrafluoroethane) | - | Carbonate (61% dolomite and 39% calcite) | • Contact angle<br>• Spontaneous imbibition | [61] |
| Fluorinated nanofluid | Water | Prepared (synthesis) calcite samples | • Dynamic and static contact angle | [62] |
| Surfapore M nanofluid | Water-based | Calcite rock | • Contact angle<br>• Spontaneous imbibition | [63] |
| Fluorinated surfactant | Toluene | Dolomite/calcite carbonate rock | • Contact angle<br>• Surface tension<br>• Adsorption | [64] |

This research focuses on the application of wettability alteration to improve recovery from gas condensate reservoirs and evaluates the efficiency of the FS-NP chemical treatment agent in gas condensate reservoirs through capillary rise tube, SI, coreflooding experiments, and measuring the decrement of trapped gas and condensate. The findings of this research can be applied to improve hydrocarbon recovery in gas condensate reservoirs and therefore extend well productivity.

# 2. Material and Method

## 2.1. Materials

The experiments were conducted using a gas condensate sample obtained from Jam Petrochemical Company, distilled water, glycerol (99.5%), and diethylene glycol (99%) as the liquid phases, while air was used as the gas phase. Glycerol and diethylene glycol were supplied by Jam Petrochemical Company, while distilled water was prepared in the laboratory. The corresponding physical properties of all tested fluids are reported in Table 2.

**Table 2. Physical characteristics of the experimental fluids at 25 °C.**

| Fluid phase | Surface tension (mN/m) | Density (g/cm$^3$) | Dynamic viscosity (cP) |
|---|---|---|---|
| Distilled water | 69.90 | 1 | 0.890 |
| Glycerol | 65.40 | 1.26 | 934 |
| Diethylene glycol | 44.80 | 1.118 | 35.70 |
| Gas condensate | 20.80 | 0.715 (API=65.93) | 0.498 |
| Air | - | 0.001225 | 0.0187 |

Trichloro (perfluorooctyl) silane (TCPFOS) was used as a fluorochemical to change the contact angle of the liquids with low surface tension, which is provided by Merck Co. Commercial hydrophilic (Merck) and synthesized hydrophobic $SiO_2$ nanoparticles [65] and an anionic FS were also utilized to change the liquid repellency of the rock surface. Among the total reserves of oil and gas worldwide, approximately 60% of the oil reserves and 40%

of the gas reserves are classified as carbonate reservoirs [66]. This emphasizes the need to increase the oil and gas recovery from carbonate reservoirs. For all experiments, carbonate rock samples collected from a representative outcrop of a southern Iranian carbonate reservoir were employed. The method used to procure carbonate core samples involved drilling outcrop blocks with a core cutter machine. Prior to the experiments, the rock samples were cleaned by Soxhlet apparatus with toluene, followed by methanol, to remove residual organic and inorganic contaminants. Once cleaned, the samples were left to dry in an oven set at 90°C for one day. Carbonate core plugs were cut into thin sections for subsequent laboratory analyses. The prepared sections were polished to obtain a smooth surface and then cleaned successively with toluene, methanol, and distilled water. The untreated carbonate rock exhibited a strongly liquid-wet surface. Figure 8 shows representative carbonate core plugs. These plugs had a diameter of 3.69 cm, lengths of 6.56-7.48 cm, porosities of 19.72-24.36%, and permeabilities of 17.13-29.94 mD.



**Figure 8. Natural carbonate core.**

## 2.2. Methods

### *2.2.1. Capillary rise tube test*

The capillary rise test was introduced several decades ago [67] and has become a well-established technique for evaluating the wetting behavior of solid material surfaces [68]. In this method, capillary forces induce the spontaneous penetration of a liquid into untreated capillaries. The degree of affinity between the liquid and the capillary surface is determined from the final equilibrium position of the liquid column. In this method, a liquid spontaneously imbibes into a capillary due to surface tension. However, for a gas-wet surface, the gas-liquid interface within the capillary resists this liquid intrusion. A negative final liquid level within the capillary signifies a gas-wetting behavior. This method allows for the theoretical calculation of a contact angle based on the observed liquid level variations. The capillary rise test requires a crucial assumption: the utilization of a perfectly wetting liquid [50]. This ideal liquid would completely wet the capillary walls, allowing for an accurate determination of the geometric factor within the Washburn equation. Unfortunately, identifying a universally perfect wetting liquid remains a significant challenge [50]. Additionally, the surface properties (physicochemical) and dimensions of the capillary itself demonstrably influence the final liquid level within the tube [68-70]. These factors can introduce complexities in data interpretation and potentially lead to inaccuracies in the calculated contact angle. Figure 9 shows a sketch of a capillary rise test [48, 71, 72].

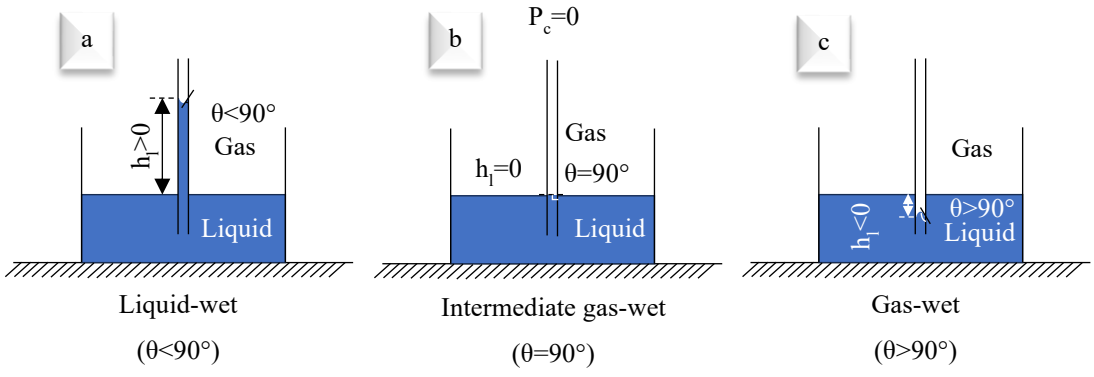


**Figure 9. Capillary liquid behavior under different wettability conditions: (a) liquid-wet with a concave meniscus, (b) intermediate gas-wet with a nearly planar meniscus, and (c) preferentially gas-wet with a convex meniscus.**

Eq. (1) is used to determine the rise or fall of the liquid column.

$$h_l = \frac{2\sigma\cos\theta}{\Delta\rho g r} \quad \textbf{(1)}$$

Eq. (1), can be used to estimate θ in a capillary tube when the liquid height ($h_l$), surface tension ($\sigma$), density difference ($\Delta\rho$), and capillary radius (r) are known. Although a contact angle of 90° is commonly regarded as the boundary between liquid-wet and gas-wet conditions, this threshold depends on pore geometry and is therefore not universally applicable. In porous media with irregular pore geometries and rough surfaces, the contact angle should be considered a qualitative rather than an absolute measure of wettability [73]. In this work, the wettability alteration to preferential gas-wetting was evaluated on two different substrates, including a capillary tube and carbonate rock. As a first step, WCA and CCA were measured on a flat glass substrate to evaluate the effect of the FS on the wettability of the glass surface properties. Glass capillary tubes with internal and external diameters of 1.1-1.2 mm and 1.5-1.6 mm, respectively, were then used for the capillary experiments. The length of the capillary tube is 75 mm. Before each experiment, the glass capillary tubes were cleaned with alcohol, rinsed thoroughly with distilled water, and dried using compressed air. The tubes were then positioned vertically in the test liquid, allowing the liquid to rise inside the capillary under capillary forces until the liquid level reached equilibrium (Figure 10). A

positive liquid height (h>0) indicated a contact angle smaller than 90°, whereas h=0 corresponded to a contact angle of 90°. A negative liquid height (h<0) indicated a contact angle greater than 90°.



**Figure 10. Capillary rise measurements in glass capillary tubes.**

After that, the capillary tube was aged in a prepared chemical solution. The aging period was 1 week at ambient temperature and atmospheric pressure. Following saturation with the chemical solution, the capillary tube was dried to remove excess chemicals from its surface. Adsorption of the chemical agents reduced the SFE, thereby converting the surface to a preferentially gas-wet state. The capillary rise of both water and condensate, as well as their SI into the air-saturated capillary tube, was measured before and after wettability alteration to evaluate the effectiveness of the surface treatment.

*2.2.2. Surface free energy*

An essential application of contact angle measurement is to evaluate the SFE of a solid. The most widely used method to determine the SFE is through the measurement of surface tension using the sessile drop method, with the unit of measurement being mN/m (dynes/cm) [74]. This method involves measuring the contact angle formed between the surface and the liquid droplet's edge. While the contact angle offers valuable information regarding the wetting properties of the surface, it is crucial to consider that the choice of liquid used for the measurements can impact the measured contact angle. The famous Young's equation (Eq. (2)) elucidates the equilibrium observed at the interface where a solid, liquid, and gas meet. The application of Young's equation relies on three key conditions. Firstly, the surface must exhibit chemical homogeneity, indicating a consistent chemical composition throughout. Secondly, the surface should be entirely flat and smooth, without any roughness or irregularities that could affect measurements. Lastly, the solid-liquid-gas system must not be influenced by gravity.

$$\gamma_{SG} = \gamma_{SL} + \gamma_{LG} \cos\theta \quad \textbf{(2)}$$

This equation relates the SFE of the solid ($\gamma_{SG}$) to the contact angle between the liquid-gas interface and the surface ($\theta$), the surface tension of the liquid phase ($\gamma_{LG}$), and the IFT between the solid and liquid ($\gamma_{SL}$). While the contact angle and surface tension of the liquid can be readily measured, the challenge lies in determining the unknown IFT ($\gamma_{SL}$), which cannot be directly measured. Over the years, several theories including OWRK/Fowkes, Wu, Acid-base, Schultz, EQS, and Zisman have been developed to address this issue and provide methods for determining the SFE of the solid [74].

Owens, Wendt, Rabel, and Kaelble (OWRK) was published in 1969 and 1970 and is one of the most common methods for SFE calculations, which is based on the Fowkes model [75-78]. The minimum number of liquids needed in this method is 2; one polar and one dispersive. The concept of decomposing SFE into individual components is based on the assumption that the $\gamma_{SL}$ arises from different intermolecular interactions governed by the properties of both the solid surface and the contacting liquid. According to the approach proposed by Fowkes, the SFE of a solid, as well as the surface tension of a liquid, can be expressed as the sum of independent components associated with specific intermolecular interactions (Eq. (3)):

$$\gamma_{SG} = \gamma_{SG}^{d} + \gamma_{SG}^{P} + \gamma_{SG}^{h} + \gamma_{SG}^{i} + \gamma_{SG}^{ab} + \gamma_{S}^{o} \quad \textbf{(3)}$$

where $\gamma_{SG}^{d}$, $\gamma_{SG}^{P}$, $\gamma_{SG}^{h}$, $\gamma_{SG}^{i}$, $\gamma_{SG}^{ab}$ denote the dispersion, polar, hydrogen-bonding, induction, and acid–base components of the SFE, respectively, whereas $\gamma_{S}^{o}$ represents all other interaction contributions. Fowkes primarily focused on solid and liquid systems in which dispersion interactions were dominant [75]. These interactions correspond to London dispersion forces generated by instantaneous fluctuations in electron dipoles. Building on Fowkes' theory, Owens and Wendt proposed that all interaction components, except the dispersion term ($\gamma_{SG}^{d}$), could be combined into a single polar component ($\gamma_{SG}^{P}$), resulting in the expression given in Eq. (4) [77].

$$\gamma_{SL} = \gamma_{SG} + \gamma_{LG} - 2\sqrt{\gamma_{SG}^{d}\gamma_{LG}^{d}} - 2\sqrt{\gamma_{SG}^{p}\gamma_{LG}^{p}} \quad \textbf{(4)}$$

372 And if Eq. (4) is combined with Young's equation, an equation called OWRK can be written
373 as Eq. (5).

$$\sqrt{\gamma_{SG}^{d}\gamma_{LG}^{d}}+\sqrt{\gamma_{SG}^{p}\gamma_{LG}^{p}}=0.5\gamma_{LG}\left(1+\cos\theta\right) \quad \textbf{(5)}$$

374 Since Eq. (5) contains two unknown parameters, $\gamma_{SG}^{d}$ and $\gamma_{SG}^{p}$ contact angle measurements
375 must be performed using two liquids with known dispersive (non-polar) and polar surface
376 tension components [74]. Ideally, one liquid should possess a dominant polar component,
377 whereas the other should be primarily dispersive. Commonly used polar liquids include
378 water, glycerol, and formamide, while diiodomethane and α-bromonaphthalene are typically
379 employed as dispersive liquids. Among these, water and diiodomethane are the most widely
380 used pair. Water is generally preferred because of its high polar contribution, ready
381 availability, and low toxicity. In contrast, selecting a suitable dispersive liquid is more
382 challenging, as many available non-polar liquids exhibit very low surface tensions, often
383 resulting in contact angles close to zero on most solid surfaces. To calculate the SFE of the
384 rock, the $\gamma_{S}^{d}$ and $\gamma_{S}^{p}$ parameters can be calculated using Owens's two-liquid method by Eq.
385 (6) and Eq. (7) [79].
386

$$\sqrt{\gamma_{SG}^{d}\gamma_{L_1G}^{d}}+\sqrt{\gamma_{SG}^{p}\gamma_{L_1G}^{p}}=0.5\gamma_{L_1G}\left(1+\cos\theta_{L_1}\right) \quad \textbf{(6)}$$

$$\sqrt{\gamma_{SG}^{d}\gamma_{L_2G}^{d}}+\sqrt{\gamma_{SG}^{p}\gamma_{L_2G}^{p}}=0.5\gamma_{L_2G}\left(1+\cos\theta_{L_2}\right) \quad \textbf{(7)}$$

387 To use more liquids and achieve more accurate data, Eq. (6) or Eq. (7) can be deconstructed
388 to provide a linear equation in the form y = mx + c (Eq. (8)) [80].

$$\frac{\gamma_L(1+\cos\theta)}{2\sqrt{\gamma_L^d}} = \sqrt{\gamma_S^p}\cdot\sqrt{\frac{\gamma_L^p}{\gamma_L^d}} + \sqrt{\gamma_S^d} \quad \textbf{(8)}$$

389 Here, the disperse component ( $\gamma_S^d$ ) and the polar component ( $\gamma_S^p$ ) of the SFE of the solid are

390 included in the intercept *c* and the slope *m*, respectively (see Figure 11).

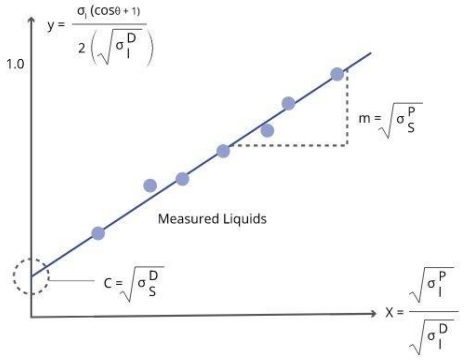



**Figure 11. OWRK plot used to determine the dispersive and polar components of SFE from the slope and intercept of the best-fit line according to Eq. (8).**

391 To determine $\gamma_S$ using Eq. (8), it is necessary to measure the contact angle using two or more

392 test liquids that $\gamma_L^d$ and $\gamma_L^p$ are already known. Note that $\gamma_S$ (SFE) is the sum of the dispersive

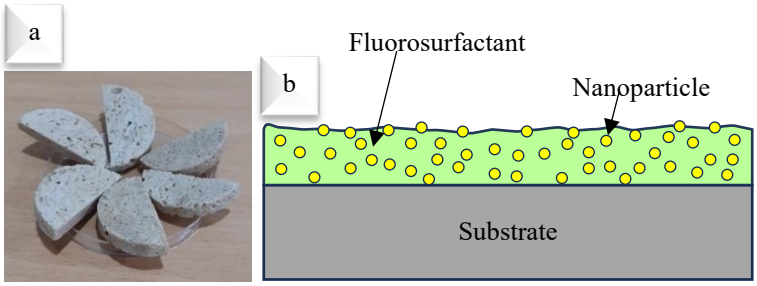
393 force and the polar force and is calculated using Eq.(9).

$$\gamma_S^{tot} = \gamma_S^d + \gamma_S^p \quad \textbf{(9)}$$

394

395 *2.2.3. Wettability alteration of thin sections*

To perform contact angle measurements on the untreated and coated thin sections of the core samples (Figure 12a and Figure 12b, respectively), core samples with a diameter of 3.5 cm were first sectioned into 4 mm thick slices using a trimming machine. The resulting specimens were polished with a grinder to obtain flat and relatively smooth surfaces. The prepared plates were then sequentially cleaned with toluene and methanol, rinsed with distilled water, and oven-dried at 60 °C for 24 h. Subsequently, the samples were immersed




in a chemical treatment solution contained in sealed glass vessels and aged under the specified temperature and exposure time defined by the experimental design described in the following section. After the aging process, the samples were removed from the solution and dried overnight at 80 °C prior to contact angle measurements.

**Figure 12. (a) Thin sections of carbonate rock, and (b) Wettability alteration on the thin sections.**

*2.2.4. Wettability alteration of the core sample (Wettability alteration at $S_{Li}$=0)*

To conduct gas-liquid (water or condensate) SI tests and core flooding experiments after wettability alteration, it was necessary to treat core plug samples. The setup for chemical treatment was similar to that used in the fluid flow test, i.e., a coreflooding apparatus. The treatment apparatus consisted of a stainless-steel aging chamber, a pressure cylinder

equipped with a movable piston, and a syringe pump connected to the piston for pressure application. The aging chamber was connected to a vacuum pump at one end and to the pressure cylinder at the other. The entire assembly was placed inside an oven to maintain the desired treatment temperature when required. The dynamic treatment process involved placing an air-saturated core in a core holder with an overburden pressure of 800 psi using the manual hydraulic pump and a back pressure of 3 bar. Then evacuating the core plugs using a vacuum pump in the core holder of the core flooding setup for two hours. Subsequently, the inlet valve was connected, and 5 PVs of the chemical solution (which was prepared based on an optimum concentration of 5 wt%) were injected at a rate of 0.05 cc/min in 5 intervals with a resting time of 12 h to ensure complete saturation of the rock with the chemical solution. Samples were collected from the outlet of the core holder at regular intervals of 0.5 PV to conduct the solid percent test (solid content) and EC test. After the treatment was completed, approximately 25-30 PVs of water injection (Q=1 cc/min) followed by dry nitrogen gas injection (Q=10 cc/min) to remove the residual chemical solution and water from the core [81]. Water was used to preliminarily evaluate the durability of the surface treatment by determining whether the adsorbed chemicals could be removed or dissolved upon exposure to water. The treated core was subsequently dried at 80 °C for 24 h in an oven to eliminate excess moisture and prepare it for the subsequent imbibition and injection tests on the treated rock sample. The weight of the core was verified to ensure that all surfactant solution was displaced. The amount of adsorption is determined by calculating the weight difference before and after the treatment, as mentioned in Eq. (10) [36].

$$C = \frac{W_{\text{after treatment}}}{W_{\text{befor treatment}}} \quad \textbf{(10)}$$

The treatment solution needs to remain stable when exposed to both water and condensate. It should not form any precipitates and must not cause a decrease in the rock's permeability. Therefore, following the modification of wettability, the absolute permeability was re-measured to determine whether any changes had occurred. A slight decrease in permeability is expected as a result of chemical adsorption onto the pore surfaces.

*2.2.5. Solid content during the wettability alteration process*

Solid content is defined as the proportion of solid material contained in a liquid or semi-liquid sample. It is quantified by placing a known amount of the sample in a weighing dish and drying it to constant weight, thereby removing all moisture and leaving only the solid residue. Then, the weights obtained before and after the drying process were recorded. The solid content was measured using a gravimetric method. Empty weighing dishes were initially weighed to the nearest 0.001 g (A). Approximately 5 g of the liquid sample was added to each dish, and the combined weight was recorded (B). The samples were then dried at 60°C for 24 h before being reweighed to obtain the final dry weight (C). The solid content was then calculated using Eq. (11).

$$Solid\ \% = \frac{Net\ weight\ of\ the\ dry\ specimen}{Net\ weight\ of\ the\ original\ specimen} \times 100 = \frac{C - A}{B - A} \times 100 \quad \textbf{(11)}$$

By collecting samples at specific intervals, you can assess how the solid percentage changes as the fluid flows through the rock. The reduction in the solid content of the effluent fluid with each injected pore volume (PV) was considered to represent the amount of adsorption.

453

454 *2.2.6. Spontaneous gas-liquid imbibition*

455 The SI test is considered one of the classical dynamic methods used to investigate the process
456 of how liquids are imbibed into a core material, and is superior to the static methods [82, 83].
457 SI refers to the process in which a wetting fluid is naturally drawn into a porous medium
458 initially saturated with a non-wetting fluid, displacing the latter solely under the action of
459 capillary forces [71]. This dynamic process is a widely employed experiment for examining
460 the alteration of wettability and the wetting state of core plugs [56-58, 84, 85]. In gas
461 condensate reservoirs, SI can be influenced by changes in capillary forces [50]. Figure 13
462 illustrates the experimental setup used to measure the SI of liquids in an air-saturated
463 carbonate core. For liquid imbibition measurement, the rock sample is air-saturated and
464 completely submerged in a liquid container (water or condensate). The SI process was
465 monitored by continuously measuring the change in the apparent weight of the core plug after
466 immersion in the test liquid. Weight variations caused by liquid uptake were recorded as a
467 function of time until equilibrium was reached. The core sample is weighed after the
468 imbibition test to determine the final average liquid saturation. The continuous weight-
469 change data acquired during SI were validated by the final liquid saturation determined from
470 the core weight at the end of the experiment.

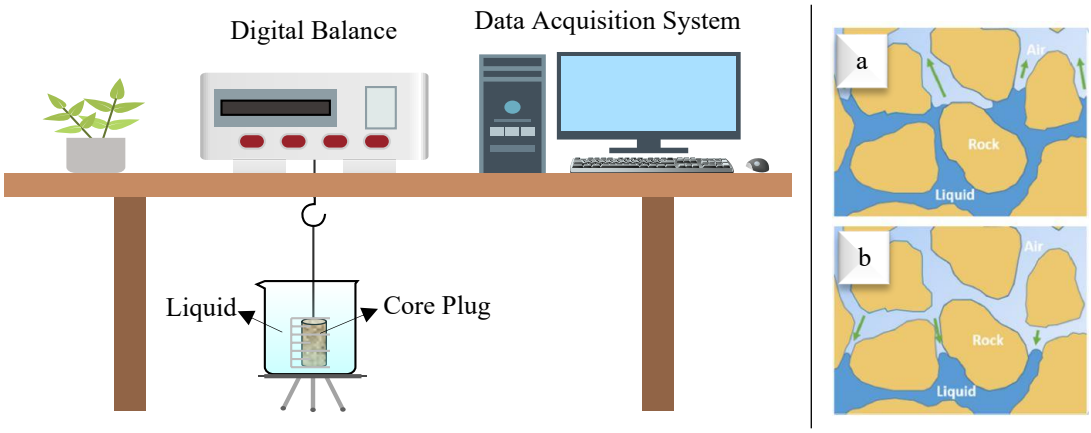



**Figure 13. Schematic of liquid-gas SI setup, (a) Imbibition in the untreated core, characterized by a concave interface, where the capillary force acts as a displacing force for liquid flow, and (b) Imbibition in the treated core, exhibiting a convex interface, where the capillary force acts as a resistance force against liquid flow.**

At first, the spontaneous water imbibition into the air-saturated rock was conducted on the untreated cores. Then, the core was washed through the soxhelet method and then dried at 90 °C for 24 h. Next, condensate imbibition was done. After that, the core was washed again and dried at 90 °C for 24 h. For the treatment of the core, the chemical agent solution was injected into the core, and the chemical agent flooding was performed for 1 week, which was explained in detail in section 3.6.2. Then, the core was dried at 80 °C for 24 h in the oven to evaporate the excess liquid. All imbibition experiments were done at 25 °C and atmospheric pressure. Next, the SI tests were done for the treated core. The recorded mass data were converted to liquid volume using the corresponding fluid density, and the imbibition behavior was reported as cumulative imbibed volume versus time. The liquid saturation was then determined according to Eq. (12) [86]:

$$S_{\mathrm{Im}b}(\%) = \frac{V_{\mathrm{Im}b}}{PV} * 100 \quad \textbf{(12)}$$

The SI results obtained for the water–air and condensate–air systems were analyzed using the analytical model of Li and Horn to quantify the reduction in liquid permeability resulting from wettability alteration toward gas-wetting conditions. The model assumes that the imbibition rate varies inversely with gas recovery [87]. In this model, the SI rate is proportional to the reciprocal of the gas recovery. By creating an appropriate plot, it is possible to estimate the permeability and capillary pressure of the liquid. The model is formulated as Eq. (13) to Eq. (16).

$$Q_L = \frac{dN_{Lt}}{dt} = a\frac{1}{\eta} - b \quad \textbf{(13)}$$

where

$$a = \frac{Ak_L\left(S_{Lf} - S_{Li}\right)}{\mu_L L} P_c \quad \textbf{(14)}$$

and

$$b = \frac{Ak_L}{\mu_L}\Delta\rho g \quad \textbf{(15)}$$

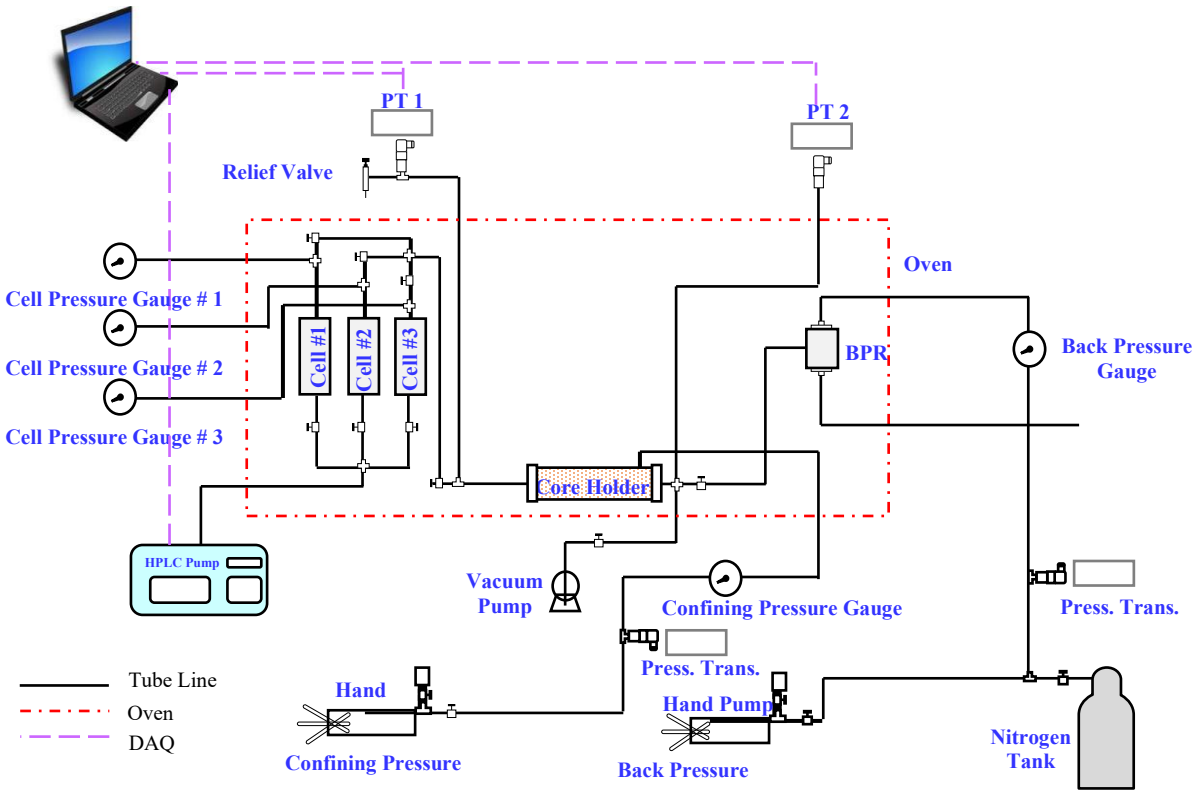
and

$$\eta = \frac{N_{Lt}}{V_p} \quad \textbf{(16)}$$

where $Q_L$ *(m³/s)* and $N_{Lt}$ are the liquid imbibition rate and the volume of liquid imbibed into the core, respectively; $A$ *(m²)* is the cross-section area of the core, $\mu_L$ *(kg/m.s)* is the viscosity of liquid, $k_L$ *(m²)*, $P_c$ *(kg/m.s²)*, $S_{Lf}$, and $S_{Li}$ are usually defined as the effective permeability of liquid, the capillary pressure, the final and initial water saturation ($S_{wi}$ and $S_{wf}$),

500 respectively; $L$ *(m)* is the core length, $\Delta\rho$ (kg/m$^3$) and g (m/s$^2$) are density difference and the
501 gravitational acceleration, respectively; $t$ is the imbibition time $V_p$ is PV of the core sample
502 and $\eta$ represents the gas recovery achieved by water imbibition, expressed in PV. Eq. (13).
503 is applicable to co-current spontaneous water imbibition into gas-saturated rocks under
504 piston-like displacement conditions. According to this model, the SI rate exhibits a linear
505 relationship with the inverse of the gas recovery (Eq. (13)). The straight line does not have
506 to pass through the origin. In fact, the intersection point of this line on the water imbibition
507 rate axis is expected to have a negative value.
508
509 *2.2.7. Core flooding procedure*
510 Core flooding experiments provide a reliable laboratory-scale approach for evaluating the
511 performance of secondary and tertiary enhanced oil recovery (EOR) techniques. The fluid
512 mobility enhancement, which is the ultimate purpose of the wettability alteration process in
513 a gas condensate reservoir, was investigated by coreflooding tests. This test was conducted
514 to evaluate the effect of the injected chemical agent on the pressure drop across the core and
515 its permeability. Wettability alteration in the coreflooding experiment was performed using
516 the optimized chemical solution obtained through the contact angle measurements.

The core flooding apparatus is capable of operating at temperatures up to 300°C and pressures up to 10,000 psi. The schematic of the core flooding setup for the displacement test is shown in Figure 14. The experimental setup consisted of a positive displacement pump capable of injecting fluids in either constant-flow-rate mode or constant-pressure mode, with a flow-rate range of 0.0001–9 $cm^3$/min and a maximum operating pressure of 700 bar. The system also included a core holder designed to accommodate core plugs with a diameter of 1.5 in. and a length of up to 7 in. Flow distributors were installed at both the inlet and outlet of the core holder to ensure uniform fluid distribution. A viton rubber sleeve surrounded the core plug and was hydraulically compressed to provide a leak-tight seal, ensuring that the injected fluid flowed exclusively through the porous core and eliminating any flow through




the annular space between the core plug and the core holder. In addition, the setup comprised a temperature-controlled oven, three fluid accumulators, high-pressure tubing and valves, a

back-pressure regulator, and a differential pressure transducer with an accuracy of ±0.25% for monitoring the pressure drop across the core. Pressure ports located at the inlet and outlet of the core holder continuously recorded the inlet and outlet pressures throughout each flooding experiment. All experiments were conducted at atmospheric pressure and ambient temperature.

**Figure 14. Schematic of core flooding apparatus**

A clean, air-saturated core plug was placed inside the core holder and sealed with end caps. Hydraulic water was introduced into the annular space between the Viton sleeve and the core holder to generate the confining (overburden) pressure. Throughout the experiments, the confining pressure was maintained at 500–700 psi higher than the injection pressure to ensure complete sealing of the core plug and eliminate any bypass flow around the core. These experiments were conducted at 25°C, and the outlet was opened to the atmospheric pressure, and for chemical treatment flooding, the back pressure was applied. For the elimination of the gravity effect, the cylinder was placed horizontally in all flooding tests. Subsequently, water or condensate was injected into the initially air-saturated core plug at a constant flow rate. Throughout the flooding experiments, the differential pressure across the core was continuously recorded by the data acquisition system, while the produced gas and liquid volumes were separated and measured using a gas–liquid separator.

# 3. Results and discussion

## 3.1. Surface free energy

SFE is one of the most important surface properties controlling the wettability of reservoir rocks, as it governs the interfacial interactions between the rock surface and the contacting fluids. It is a critical factor in determining how well a liquid can spread and adhere to the surface [88]. To evaluate the wettability alteration of the rock, its surface free energy (SFE) was measured. For this purpose, we have measured contact angles by the static sessile drop method using a contact angle measurement setup. The used liquids were condensate as a non-polar and distilled water as a polar or dispersive liquid. The OWRK method is one of the most widely adopted approaches for determining the SFE of solid surfaces from contact angle measurements using multiple probe liquids with known surface tension components. The surface tension values, together with their polar and dispersive components, for the selected reference liquids are presented in Table 3.

**Table 3. Surface tension ($\gamma_{LG}$) of test liquids, their dispersive ($\gamma sd$) and polar ($\gamma sp$) components.**

| **Liquid** | $\gamma_{LG}\,(mN/m)$ | $\gamma_{LG}^{d}\,(mN/m)$ | $\gamma_{LG}^{p}\,(mN/m)$ | **Ref.** |
|---|---|---|---|---|
| Water | 72.8 | 21.8 | 51 | [89-91] |
| Glycerol | 64 | 34 | 30 | [89] |
| Ethylene glycol | 48 | 29 | 19 | [89] |
| Condensate | 20.8 | 20.8 | 0 | This work |

The plot in Figure 15 is generated using the OWRK equation (Eq. (8)). The equations and the coefficient of determination ($R^2$ or R-squared) values are shown next to each line. The $R^2$ is a statistical metric that quantifies the goodness of fit of a linear regression model to the experimental data. In general, an $R^2$ value approaching unity indicates that the regression model provides a better representation of the observed data. In these cases, all the R-squared values are above 0.92, which indicates a good fit for a linear model.

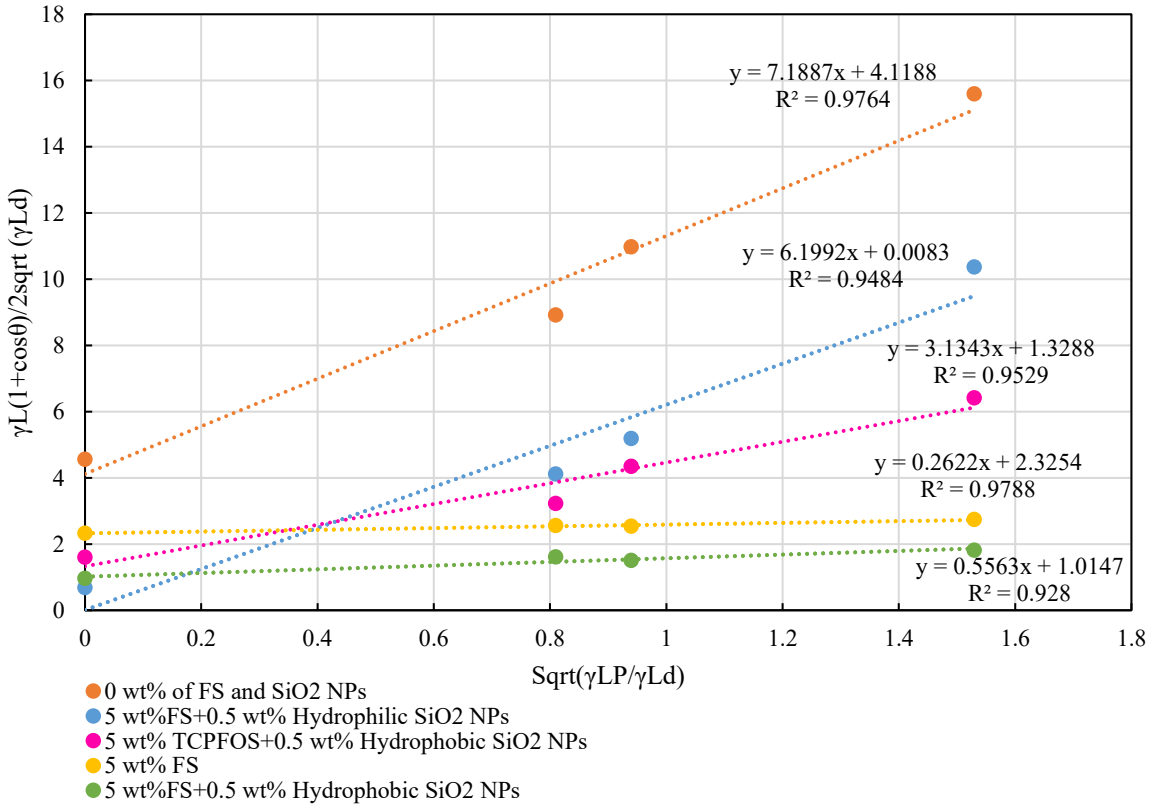
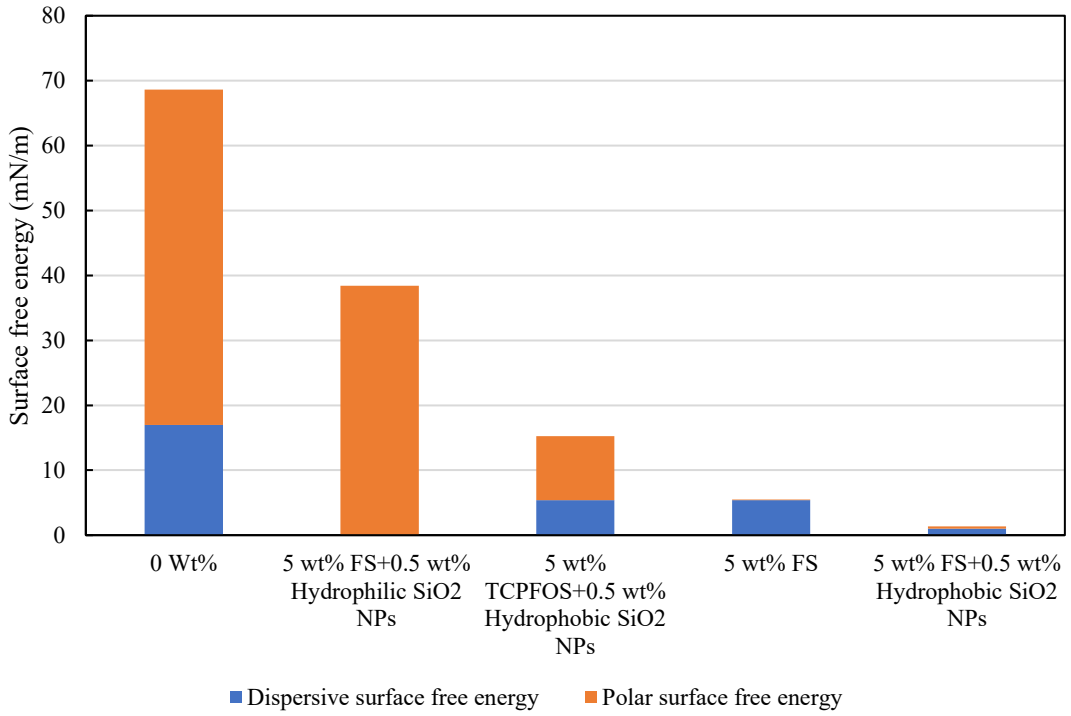



**Figure 15. OWRK plots for different chemical solution agents.**

According to the OWRK method, the slope of the regression line represents the polar component ( $\gamma_S^p$ ) of the SFE, whereas the y-intercept represents its dispersive component ( $\gamma_S^d$ ). Figure 16, which shows dispersive and polar SFE, illustrates the variation in SFE before

and after treatment with different chemical solution agents. Initially, the SFE of the carbonate rock sample was approximately 68.64 mN/m, and the contact angles of all used liquids were 0°, so the wettability of the untreated core was preferential liquid-wetting. However, after treatment with different chemical solutions, the contact angle of liquids increased and SFE decreased from 68.64 to different values reported in Table 4. The rock surface wettability had been altered from liquid-wetting to a preferential gas-wetting state. The SFE of the treated sample with the most effective solution was about 1.72 mN/m. These findings align with the contact angle measurements, supporting the notion that the used chemical agent can effectively achieve the gas-wetting state of the carbonate rock surface [92]. The surface energy is reduced as a consequence of adsorption, leading to a preferential affinity of the solid surface towards gas molecules. This means that the solid surface becomes more inclined to be wetted by gases. This result is consistent with studies by [79, 93]. According to Aminnaji et al., the wettability alteration mechanisms of SurfaPore M nanofluid involve reducing SFE by depositing fluorinated functional groups on the rock surface [57]. Similarly, Erfani Gahrooei et al. demonstrated the same phenomenon with the use of MariSeal 800 chemical [94].

591 The reduction in SFE induced by fluorinated chemical agents is attributed to the formation
592 of a fluorinated layer on the rock surface. Increasing the concentration of the chemical




593 treatment enhances the surface coverage of fluorinated species, resulting in a greater
594 reduction in SFE than that achieved at lower concentrations.

595 **Table 4. SFE of the carbonate rock after treatment with different chemical solutions.**

| Chemical solution agent | Contact angle (°) | | | | SFE |
|---|---|---|---|---|---|
| | Water | Glycerol | DEG | Condensate | (mN/m) |
| 0 wt% (Rock before treatment) | 0 | 0 | 0 | 0 | 68.64 |
| 5 wt% FS+0.5 wt% Hydrophilic $SiO_2$ NPs | 70.72 | 93.13 | 94.47 | 134.29 | 38.43 |
| 5 wt% TCPFOS+0.5 wt% Hydrophobic $SiO_2$ NPs | 100.19 | 102.00 | 106.05 | 107.30 | 15.23 |
| 5 wt% FS | 130.44 | 122.54 | 115.26 | 88.73 | 5.48 |

**Figure 1. The change of SFE using different chemical solution agents.**

| | | | | | |
|---|---|---|---|---|---|
| 5 wt% FS+0.5 wt% Hydrophobic $SiO_2$ NPs | 140.17 | 136.55 | 129.69 | 116.41 | 1.72 |

## 3.2. Capillary rise tube test

Contact angle measurements offer a large-scale view of wettability. To gain a more detailed understanding of wettability at a microscopic level, the capillary rise test is employed. Among the earliest methods for wettability characterization, capillary tube (micromodel) experiments enabled direct visual observation of fluid–solid interactions. First of all, the contact angles of water and condensate on the flat glass substrate are measured and shown in Figure 17. Upon treatment with the chemical solution, the contact angle of water on the flat glass substrate increased by a factor of 3.6, and the contact angle of condensate increased by a factor of 8.5. The small rectangular glass is immersed in the solution containing the FS for 2 days under ambient conditions.

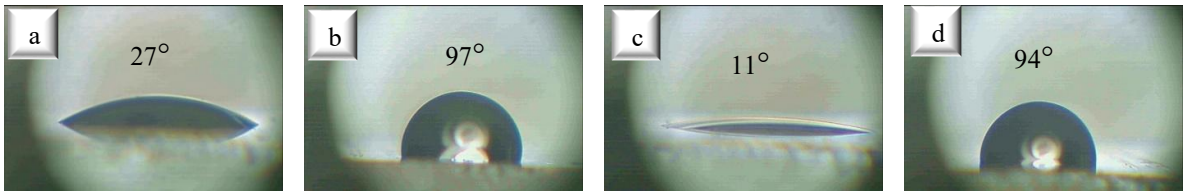



**Figure 2. Liquid droplet on the flat glass substrate, (a) Water droplet-Before WA, (b) Water droplet-After WA, (c) Condensate droplet-Before WA, (d) Condensate droplet-After WA.**

Furthermore, different tests in a capillary tube were conducted. Figure 18 presents the capillary liquid rise as a function of FS concentration for the gas–condensate and gas–water systems during chemical treatment. In both cases, the liquid rise decreased markedly as the FS concentration increased and became nearly constant once the concentration reached approximately 5 wt%. Consequently, the influence of FS concentration on the capillary rise becomes negligible once the concentration exceeds approximately 5 wt%, indicating that the treatment has reached its maximum effectiveness. Moreover, the reduction in the capillary

rise of water is considerably greater than that of condensate, indicating a more pronounced wettability alteration in the gas–water system. As the FS concentration increased, the capillary rise of water decreased significantly from 24.60 to 4.48 mm. The condensate exhibited a similar behavior, with its capillary rise decreasing from 9.98 mm to zero. These findings are in excellent agreement with the contact angle measurements, demonstrating that the observed reduction in capillary rise is directly associated with the wettability alteration induced by the fluorosurfactant treatment.

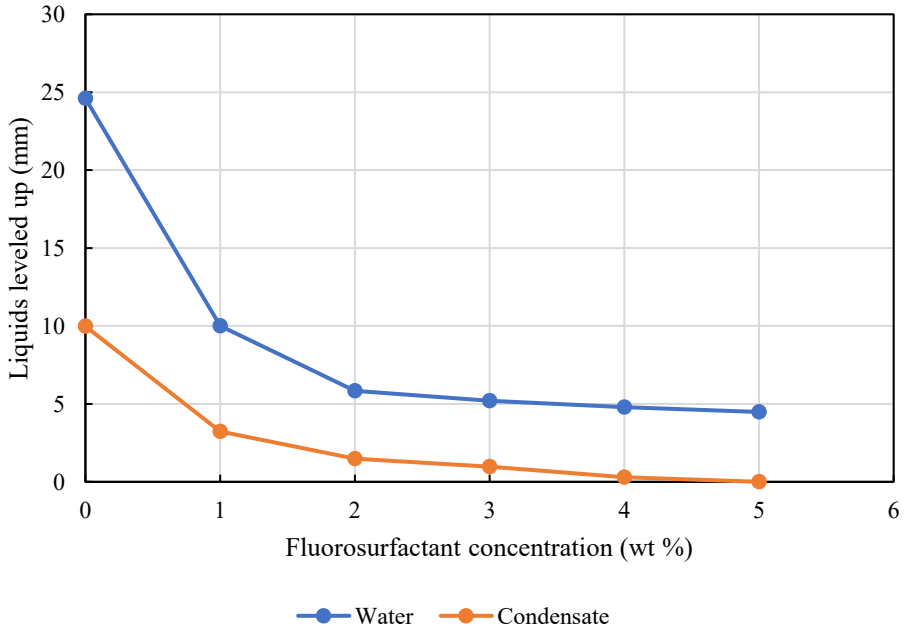



**Figure 18. Effect of fluorosurfactant (FS) concentration on the capillary rise of water and condensate.**

The contact angles and the liquid levels before wettability alteration (BWA) and after wettability alteration (AWA) with 5 wt% FS in methanol for both water and condensate are shown in Figure 19.

$$\theta = \arccos\left(\frac{\rho g h r}{2\sigma}\right) \quad \textbf{(17)}$$

Eq. (17) is obtained by balancing the capillary and gravitational forces acting on the liquid column, where σ and ρ are the liquid surface tension and density, respectively, g is the acceleration due to gravity, and r denotes the radius of the capillary tube. A decrease in capillary rise coupled with an increase in contact angle (at constant surface tension) demonstrates a transition from a strong liquid-wetting state. This observation implies a change in the wettability characteristics of the system [95].

Prior to chemical treatment, the contact angles of water and condensate in the glass capillary tube were approximately 33° and 23°, respectively. After treatment with 5 wt% FS, these values increased to approximately 73° and 90°, respectively. The increment of CCA due to the wettability alteration process in the capillary rise tube is 40° and 67° for air-water systems. These results indicate that treatment with 5 wt% FS altered the wettability of the gas–liquid–glass system to an intermediate gas-wet state. However, this method has an inherent limitation. When the capillary rise exceeds approximately 12 mm for water or 4.95 mm for condensate, the contact angle can no longer be determined accurately. Under these conditions, the calculated contact angle approaches 0°, resulting in $\cos\theta > 1$, which has no physical meaning. The results are consistent with those reported by [58]. The liquid levels of water and condensate in the capillary after treatment are approximately 4.48 and 0 mm, and the calculated contact angles of water and condensate are about 69° and 90°. The calculated contact angle of water is very near the measured value, which is 73°.

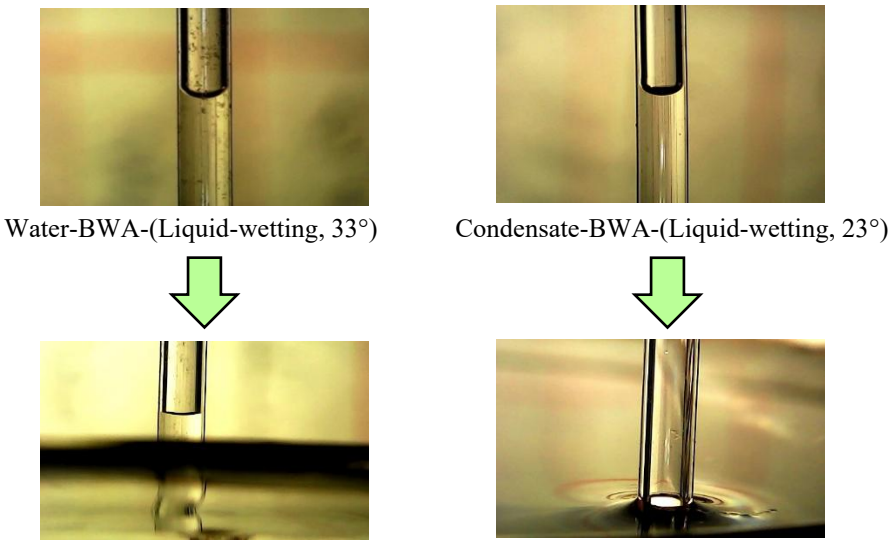



**Figure 3. Capillary rise tube test before and after wettability alteration for water and condensate.**

### 3.3. Stability of the droplet

Figure 20 and Figure 21 showed the first 15 minutes of water and condensate drop shapes and their contact angles after treatment with a qualified chemical solution. Furthermore, in Figure 22, the comparison between the stability time of water and condensate was shown. It is obvious that the change in water droplet was lower than that of condensate, and after 2 min, the water contact angle was constant and its decrement after 15 min was 15%, while it was 33% for condensate. It is worth noting that the imbibition of both water and condensate drops was rapid and complete prior to the treatment process, and the contact angle, as visually observed, was zero. These findings indicate that the chemical treatment successfully altered the wettability of the rock surface toward an intermediate gas-wet state.

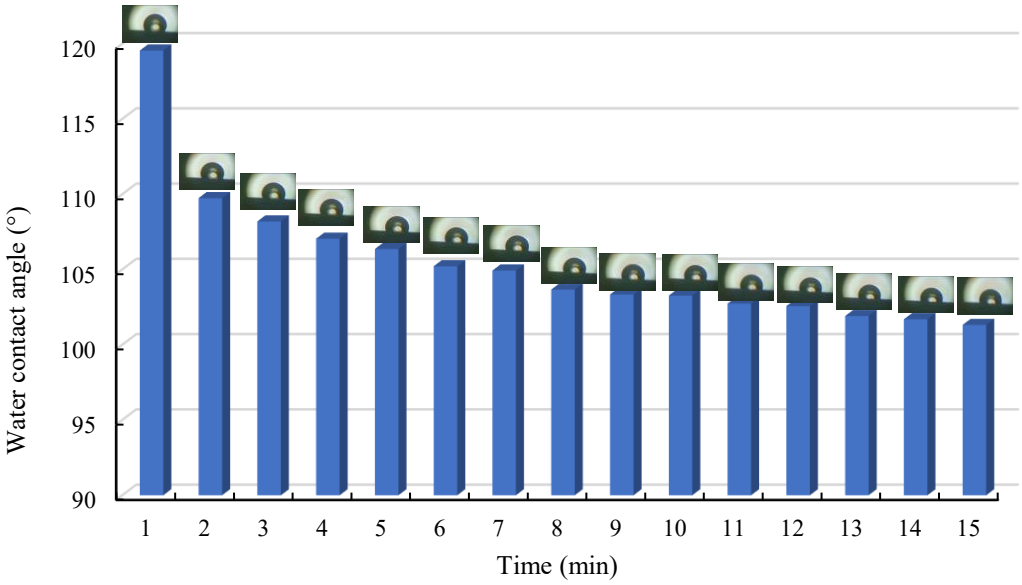
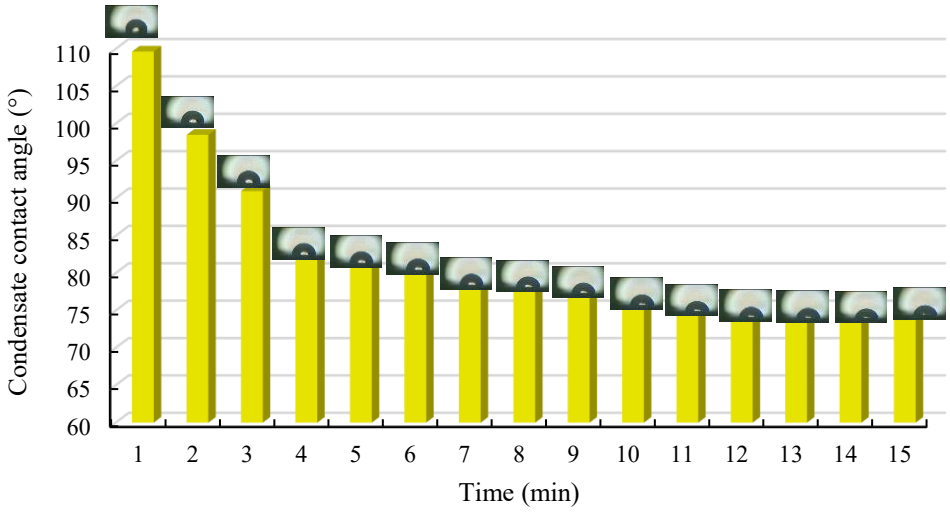
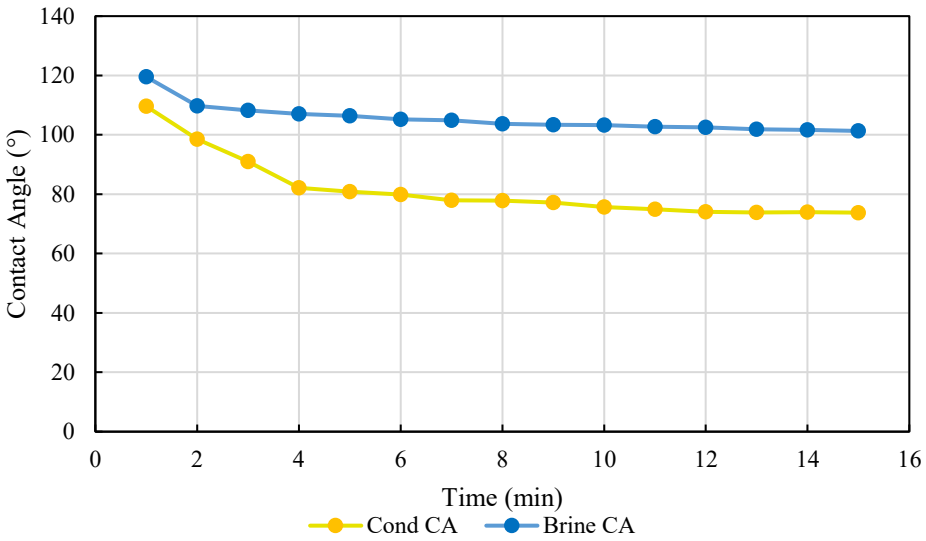



**Figure 20. Static water contact angle on a treated carbonate thin section as a function of time.**




653 **Figure 21. Static condensate contact angle on a treated carbonate thin section as a function of time.**




654 **Figure 22. Comparison between the stability time of water and condensate droplet.**

655 For another treatment process using TCPFOS-$SiO_2$ NPs, the condensate drops disappear after
656 a short time, as depicted in Figure 23. Regarding the water, the drop also imbibes relatively
657 fast after a couple of minutes. It was shown that the decrements for water and condensate
658 after 1 min were 35% (131° to 85°) and 52 % (89° to 43°), respectively. This is a drawback
659 in the WA process. So, it is not a good choice to permanently change the wettability toward
660 a gas-wetting state.

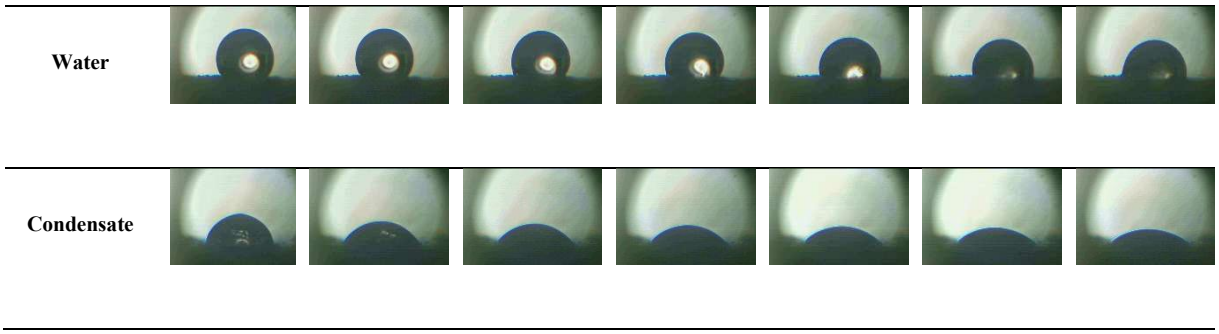


**Figure 23. Change in water and CCA during 1 min after using TCPFOS-$SiO_2$ NPs chemical solution.**

It should be emphasized that evaporation of the liquid phase may have influenced the observed contact angle variations. For more reliable results, the measurements could be extended over longer durations to capture the complete trend of contact angle evolution. Furthermore, performing the tests inside a controlled, sealed chamber to minimize evaporation effects would help ensure that the observed changes are primarily due to wettability alterations rather than fluid loss to the surroundings. Additionally, performing each measurement multiple times and presenting the averaged results with standard deviations in a bar chart format provides a more accurate comparison of wettability before and after treatment.

### 3.4. EC and solid percent values

The effectiveness of wettability alteration in improving flow depends on the flow conditions, including saturation of the rock, porosity, and permeability of the rock, flow rate, and injected PV. Analysis of the EC–PV curve provides valuable information on the adsorption capacity of the rock and the surfactant–rock interaction. For this purpose, fluid samples from the outlet were collected every 0.5 PV during chemical solution flooding in containers with a sufficiently small diameter to permit insertion of the conductivity probe and reduce sample evaporation. The flooding and measurements kept going until the conductivity remained practically unchanged with time. As the chemical solution flows through the rock sample, the surfactant starts to adsorb onto the rock surface. This leads to a decrease in the surfactant concentration in the exiting solution, causing the EC to decrease compared to the initial value

of 681 µs/cm, due to anionic FS adsorption on the rock surface. A decrease in EC followed by an increase is expected in the dynamic process. Initially, the fresh surfactant solution had a clean rock surface, leading to rapid adsorption and a significant decrease in EC. Over time, the available adsorption sites on the rock surface become progressively occupied. The rate of adsorption slows down. The concentration of surfactant in the outlet solution starts to increase, and the EC gradually rises toward the initial value as depicted in Figure 24.

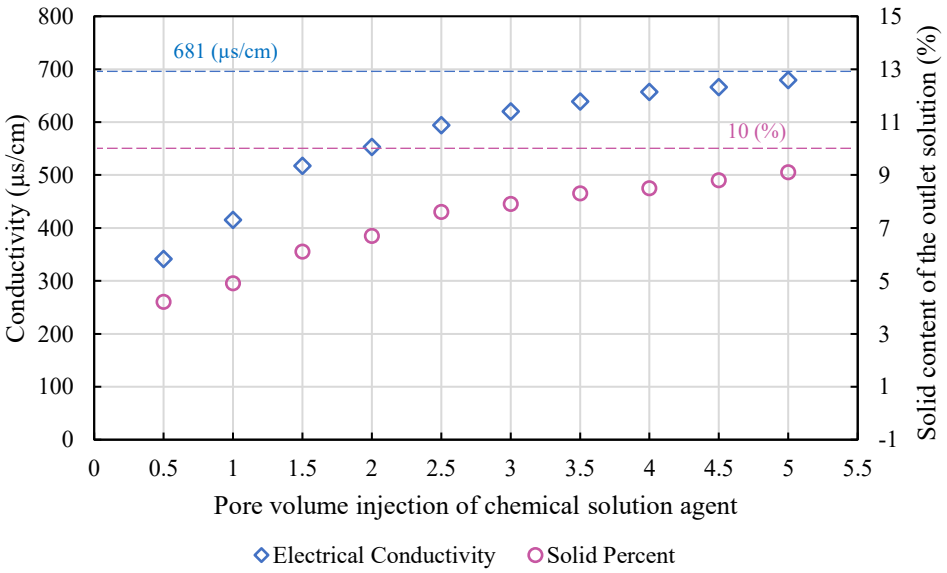


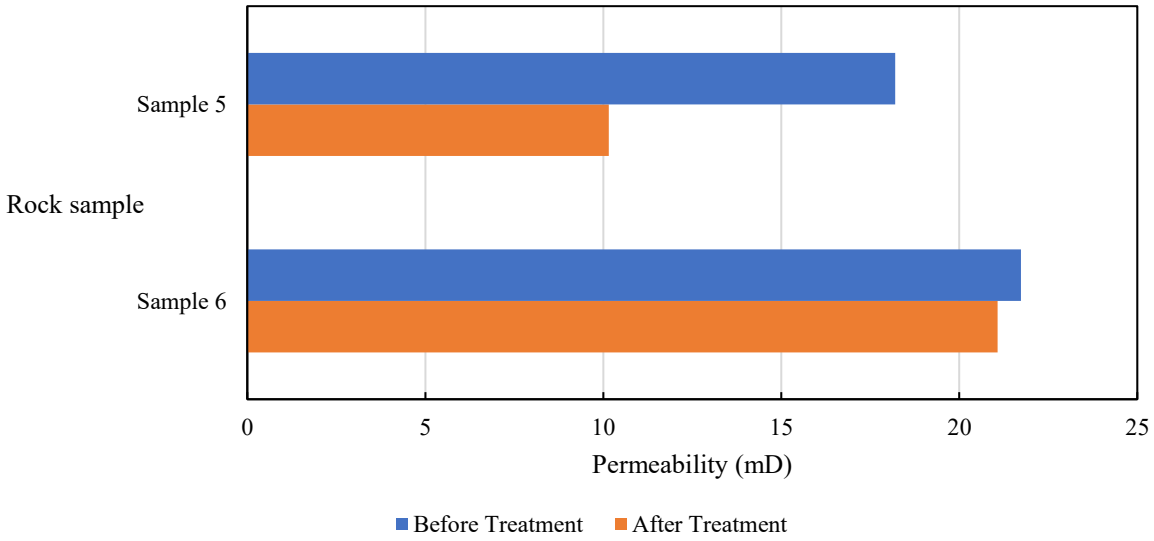

**Figure 24. Conductivity and solid% of the outlet sample during dynamic chemical solution injection.**

Furthermore, the solid content of the outlet solutions was measured. As expected, the outlet solutions initially contain few measurable solid components. Since the solid was adsorbed and remains in the core. The solid content of the outlet solutions increased slightly to around 9.1% at 5 PVs injection. By combining the trends in EC and solid content data, we can gain a more comprehensive understanding of the interaction between the rock and the chemical

694 solution. The initial decrease in EC and solid percent suggests FS adsorption into the rock
695 pores.

696 **3.5. Re-measuring absolute permeability after wettability alteration of the rock**

697 The rock permeabilities of the used samples before and after the treatment process are
698 compared in Figure 25 for both chemical agents with and without NPs, and the permeability
699 decrement due to chemical treatment is reported in Figure 26. While treatment with FS alone
700 resulted in negligible permeability impairment, the combination of FS and nanoparticles
701 (NPs) led to a significant reduction in the permeability of the carbonate rock, which is likely
702 attributable to the multilayer adsorption of nanoparticles on the rock surface [96]. Therefore,




703 FS alone appears to be a more suitable candidate for the wettability alteration of carbonate
704 rocks. It is important to note that if the permeability and pore size of the used rocks were
705 larger, the presence of NP would not significantly affect the rock permeability.

**Figure 25. Permeability of the core samples 5 and 6 before and after chemical treatment with chemical agents with and without NPs, respectively.**

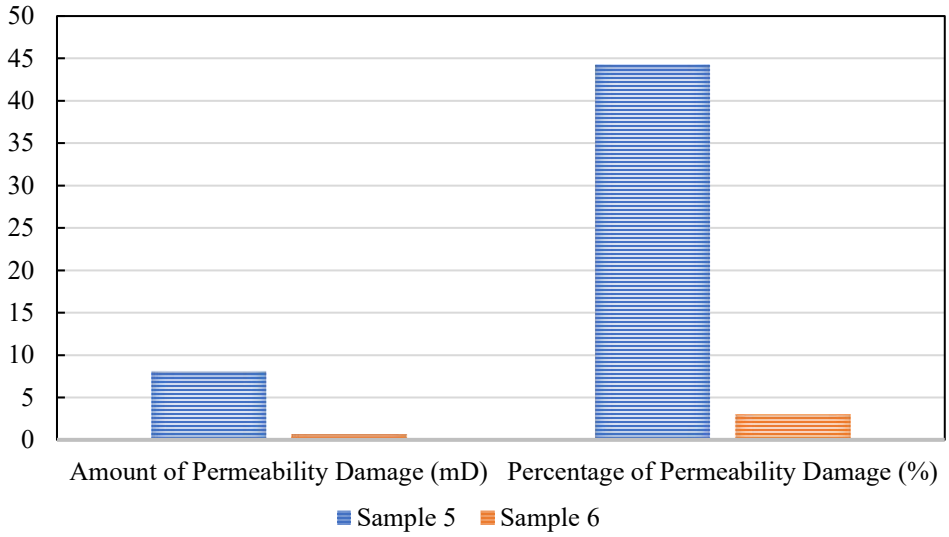



**Figure 26. Amount and percentage of permeability damage for samples 5 and 6 due to chemical treatment with chemical agents with and without NPs, respectively.**

## 3.6. Gas-liquid spontaneous imbibition

To verify the effectiveness of the chemical treatment in inducing gas wettability, gas–liquid imbibition tests were performed on carbonate plugs. The plug was connected to a balance and placed in water or condensate. The weight variations resulting from the imbibition of the liquid were recorded. The volumes of the imbibed fluids before and after chemical treatment were calculated from the weight change of the core plugs and the corresponding fluid densities. During these test series, the core samples were subjected to chemical treatment,

and then they were utilized for spontaneous imbibition testing. Figure 27 and Figure 28, show the water and condensate imbibed volume in the core versus time during spontaneous imbibition in the treated and untreated core, respectively. Untreated carbonate rock samples exhibited strong liquid-wet characteristics under gas–liquid conditions. As a result, the imbibition curve displayed a steep initial rise, reflecting the strong capillary forces that promoted rapid spontaneous imbibition during the early stage of the experiment. As time progresses, the steepness of the slope gradually diminishes, resulting in the liquid saturation of approximately 14.04% and 20.08% of the effective volume of the plug space for water and condensate after 20 minutes, respectively. The results are in line with those reported by [97].

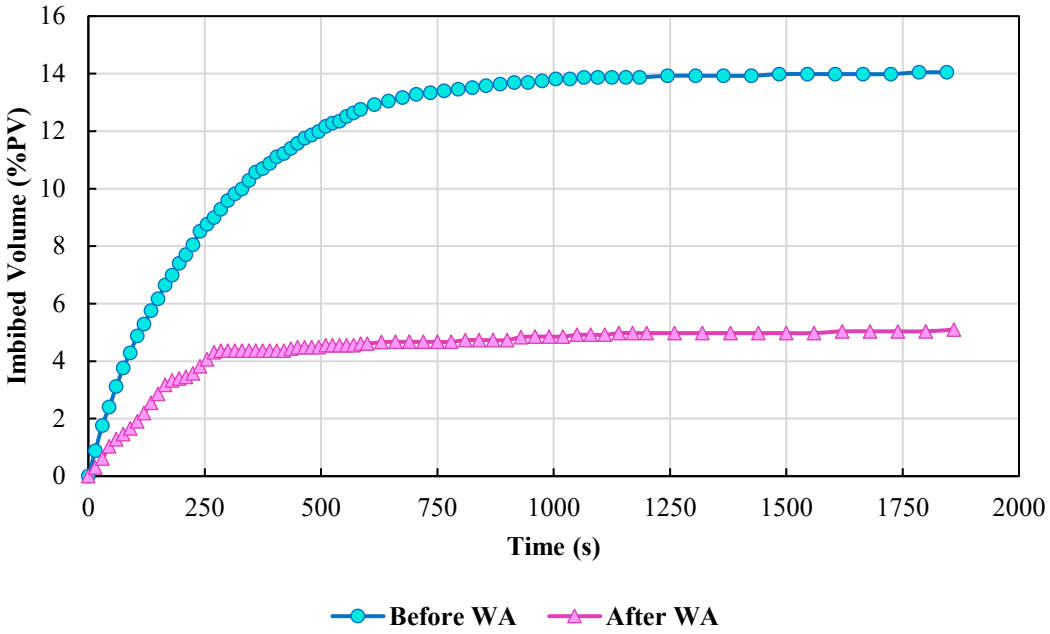



**Figure 27. Spontaneous imbibition of water before and after treatment with 5 wt% FS solution on P6.**

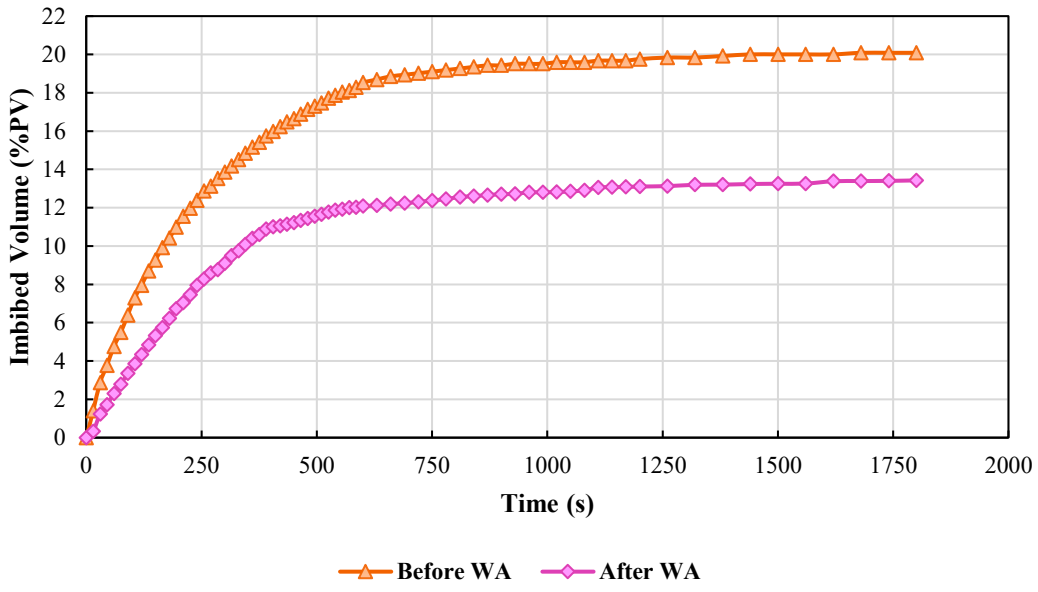


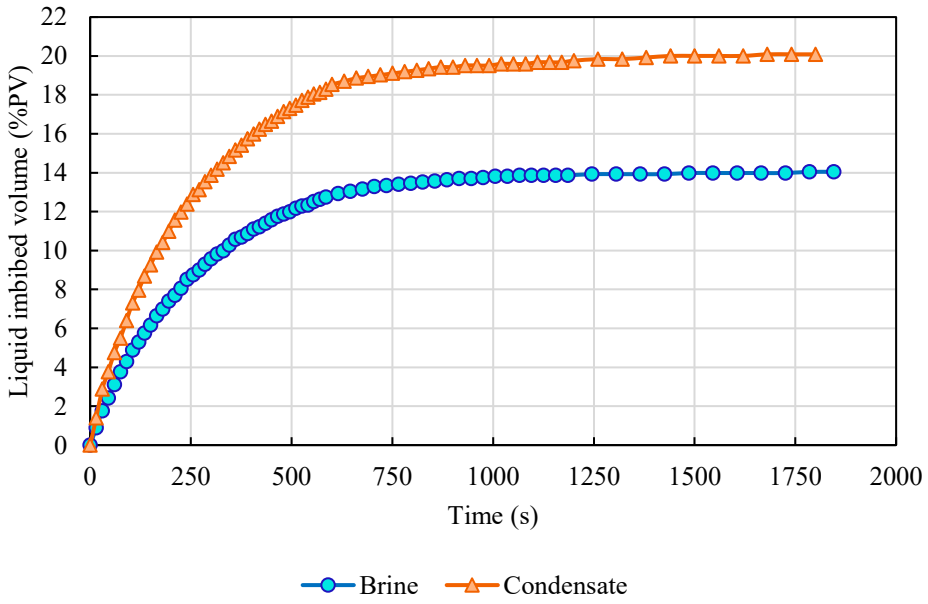

**Figure 28. Spontaneous imbibition of condensate before and after treatment with 5 wt% FS solution on P6.**

As the rock wettability shifts toward a gas-wet state, liquid imbibition into the rock decreases [57, 98]. This trend was consistently observed in both gas–water and gas–condensate systems. Accordingly, the reduction in the imbibition rate and the ultimate liquid recovery following chemical treatment serve as an indicator of the degree of wettability alteration. Before the treatment, since the core is strongly liquid-wet, the imbibition of water and condensate was 14.04% PV and 20.08% PV at the test termination, respectively. After treatment, these values decreased to 5.09% PV and 13.42% PV for water and condensate, respectively. Therefore, the liquid saturation is reduced by about 63.75% for water and 33.17% for condensate after the treatment. However, the impact on condensate imbibition is not as notable as the effect observed in water imbibition. The imbibition measurements

suggest that the core plug strong affinity to liquids was reduced following the chemical treatment. Therefore, the untreated rock had a preference for liquids, but the treatment altered its wettability to favor gas, which could potentially facilitate the elimination of liquid blockages in gas condensate reservoirs. Compared with the unaged core, the aged core exhibited an earlier decline in the imbibition rate. This indicates that not only the final liquid saturation in the core but also the rate of imbibition demonstrates a favorable change in wettability due to the treatment. This occurs because imbibition relies on the wettability characteristics of the rock.

A brief explanation for this observation is provided here. The spontaneous liquid imbibition shown in Figure 13 is governed by the balance between capillary and gravitational forces. Capillary pressure drives the imbibition process, whereas gravitational forces resist the upward movement of the liquid. The force of gravity remained constant throughout the spontaneous imbibition process, regardless of whether the chemical treatment was applied or not. Therefore, the observed decrease in recovery during spontaneous liquid imbibition can be attributed solely to the alteration in capillary pressure. The change in capillary pressure, caused by the wettability modification induced by the chemical treatment, is the primary factor contributing to the reduction in SI. The chemical treatment had minimal impact on surface tension, porosity, and permeability. However, the analysis indicates that the observed reduction in spontaneous imbibition recovery results from wettability alteration, as reflected by the increase in contact angle. An increase in contact angle reduces the capillary pressure, thereby suppressing spontaneous liquid imbibition into the pore space. This behavior confirms that the chemical treatment altered the rock wettability from a liquid-wet to a gas-wet state. This result was consistent with the analysis of contact angle SFE and the capillary

762 rise tube test. It is noteworthy that the modification of wettability is aimed at reducing the
763 tendency of the surface to be liquid-wet.
764 While there are similarities between condensate imbibition and water imbibition in terms of
765 the process of fluid that is drawn into the porous structure of the rock, there are also important
766 differences. One key difference is the nature of the fluids involved. The difference in surface
767 tension between water and condensate plays a vital role in the imbibition behavior of these
768 fluids in a liquid-wet rock. Figure 29 compares the spontaneous imbibition of water and
769 condensate in the untreated core sample (P6), demonstrating that condensate imbibed into
770 the air-saturated core to a much greater extent than water, which is in good agreement with
771 previously published results [31, 36, 41, 72].




772 **Figure 29. Spontaneous imbibition of water and condensate before treatment in the P6 core sample.**

773 This behavior may be attributed to the stronger oil-wet tendency of the rock in gas–oil–rock
774 systems compared with its water-wet tendency in gas–water–rock systems. Since the rock

surface has a preference for the condensate phase over water, more effective imbibition of the condensate into the core is observed. The condensate can penetrate and fill the pore spaces of the rock more readily than water due to its wetting characteristics. Furthermore, condensate has a lower IFT with the rock surface compared to water. A lower IFT between the condensate and the rock surface allows for better wetting and easier penetration into the porous structure of the core, resulting in higher imbibition compared to water. This behavior can be explained by the role of capillary pressure, the dominant driving force governing spontaneous imbibition, which becomes stronger as the affinity of the rock surface for the imbibing fluid increases. These results are consistent with those reported by Fahes and Firoozabadi [36] and agree well with the contact angle measurements, which show that the contact angle measured through the liquid phase is smaller in gas–oil systems than in gas–water systems.

Although the thin section contact angle analysis indicated a fully gas-wet surface after treatment, the core scale tests still showed a minor spontaneous imbibition response. This is not contradictory; it reflects the fact that wettability alteration at the pore network scale is rarely perfectly uniform. In thin sections, the rock surface is completely immersed in the treatment solution, ensuring full chemical coverage under static conditions. In contrast, during core treatment, fluid transport into the internal pore space occurs via advective and diffusive processes that are influenced by pore size distribution, tortuosity, and mineral heterogeneity. As a result, some micropores or low-permeability regions may receive insufficient exposure to the chemical treatment agent, retaining partial water-wet characteristics.

From a reservoir engineering standpoint, the observed residual imbibition does not indicate a failure of the treatment. The accumulation of condensate around the wellbore is one of the main factors responsible for production decline in gas-condensate reservoirs, as it reduces the relative permeability to gas. Achieving a perfectly uniform gas-wet condition across the entire reservoir pore space is neither technically achievable nor required for meaningful productivity gains. Field-scale effectiveness depends on the extent of wettability alteration within high-permeability networks that primarily control hydrocarbon flow. If a sufficient proportion of these critical pathways is converted to a gas-wet state, the resulting improvement in gas mobility and reduction in capillary trapping can significantly mitigate condensate blockage and enhance well deliverability, even if isolated low-permeability zones remain partially water-wet.

Figure 30 shows the rates of spontaneous water and condensate imbibition in gas–water and gas–condensate systems, respectively, expressed in %PV/min. Carbonate rock exhibits a slightly higher spontaneous imbibition rate for condensate than for water [31]. This discrepancy in imbibition rates may be attributed to the greater liquid-wetting characteristics observed in gas-oil-rock systems compared to gas-water-rock systems.

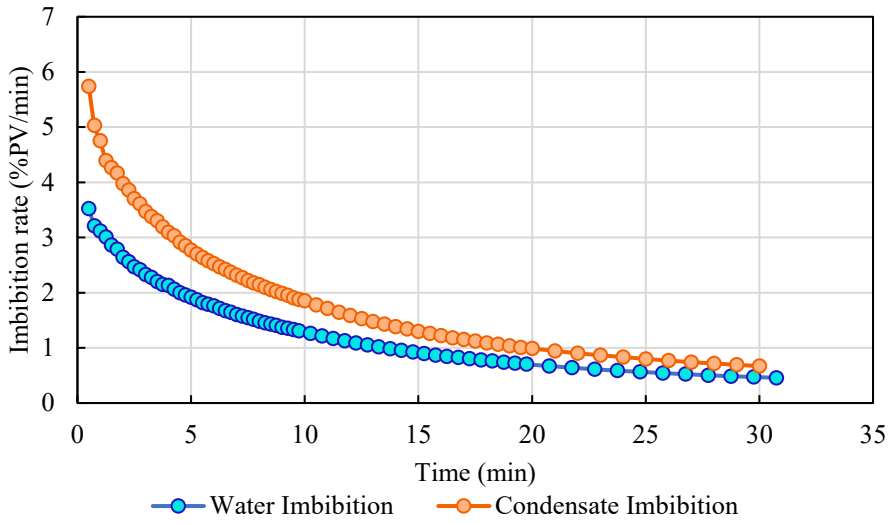
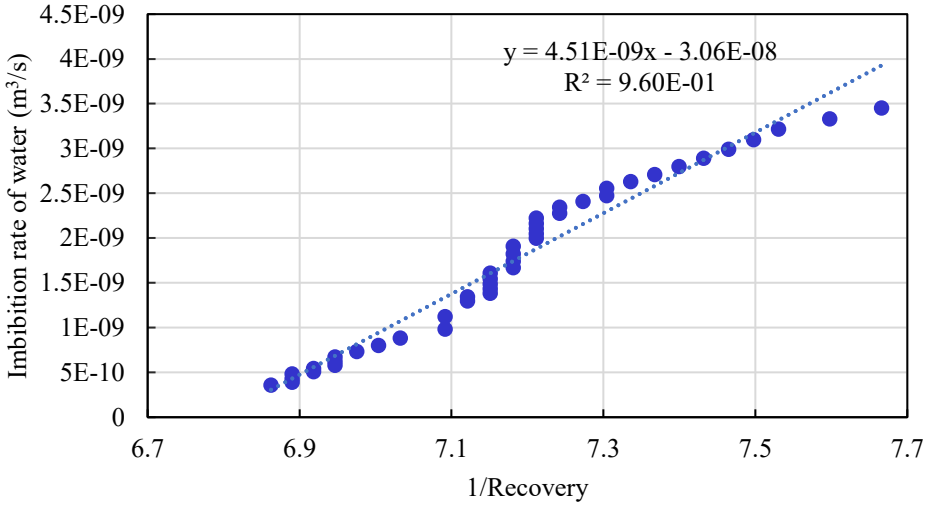



**Figure 30. Water and condensate imbibition rates for the air-saturated carbonate rock before chemical treatment**

The SI experimental data for both water and condensate were used to calculate the permeabilities of the liquid phases and capillary pressure using Eq. (13). Figure 31 and Figure 32, depict how well the Li and Horn model aligns with the experimental data. The linear equation and the $R^2$ of the model are also reported in these two figures. The permeability and




$P_c$ values of the core can be calculated using the intercept and the slope.

**Figure 31. Spontaneous imbibition rate of water versus the reciprocal of the gas recovery before wettability alteration.**

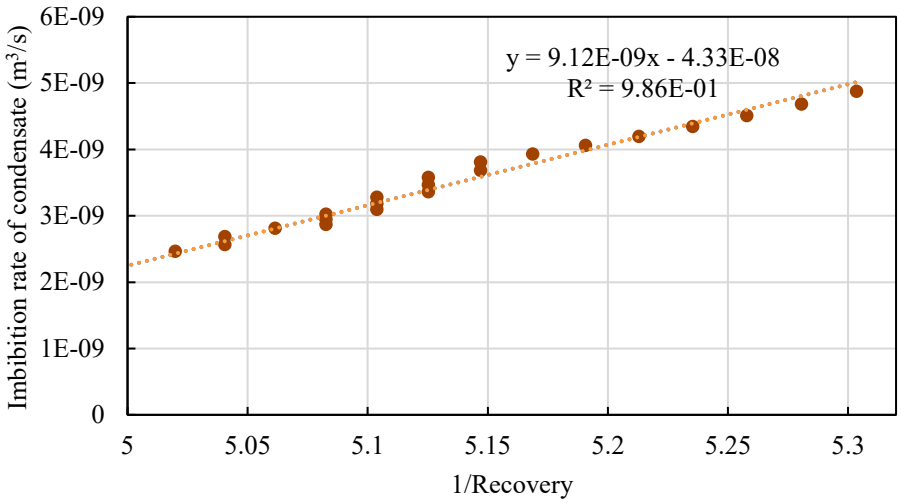



**Figure 32. Spontaneous imbibition rate of condensate versus the reciprocal of the gas recovery before wettability alteration.**

Table 5 presented the permeability and capillary pressure for both water and condensate before wettability alteration. A comparison of the results shows that the values of k and $P_c$ are very similar for the water and condensate systems because both experiments were conducted using the same carbonate core.

**Table 5. Liquid permeability and capillary pressure using spontaneous imbibition data before wettability alteration.**

| Liquid | k ($m^2$) | $P_c$ ($kg/m.s^2$) |
|---|---|---|
| Water | 2.92E-12 | 6.32E+02 |
| Condensate | 2.87E-12 | 6.77E+02 |

Figure 33 and Figure 34 depict the water and condensate imbibition rate vs. the reciprocal of the gas recovery after wettability alteration using the chemical solution. The k and $P_c$ values are also reported in Table 6. When comparing the intercepts before and after the treatment, it was observed that there was a significant decrease in water permeability by approximately 72.7%. This reduction confirms that the surface modification of the porous media by the chemical solution has led to a decreased tendency for water and condensate phases to imbibe into the porous rock. Furthermore, the calculated capillary pressure data indicate a 23.5% increase after wettability alteration.

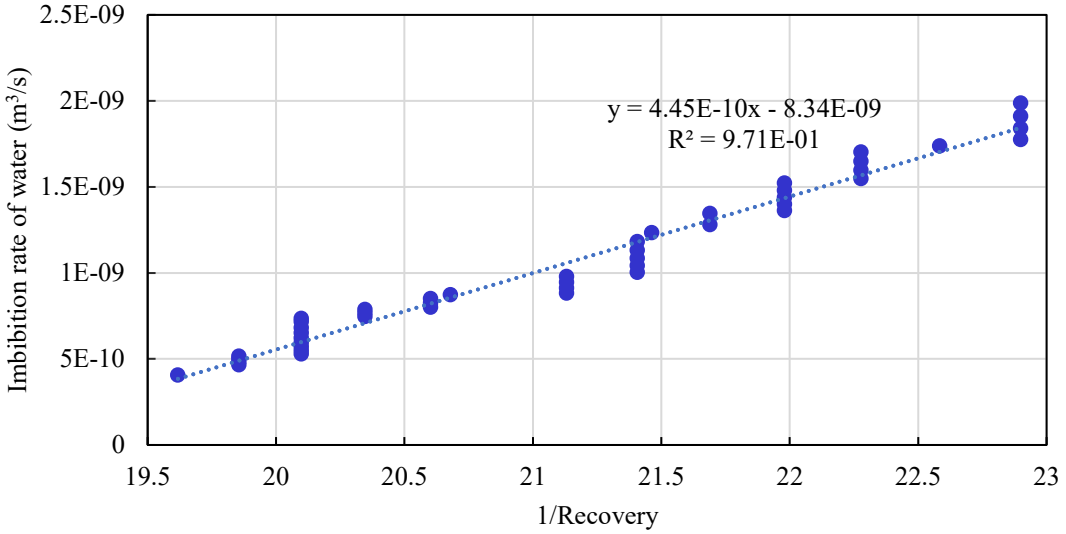



**Figure 33. Spontaneous imbibition rate of water versus the reciprocal of the gas recovery after wettability alteration.**

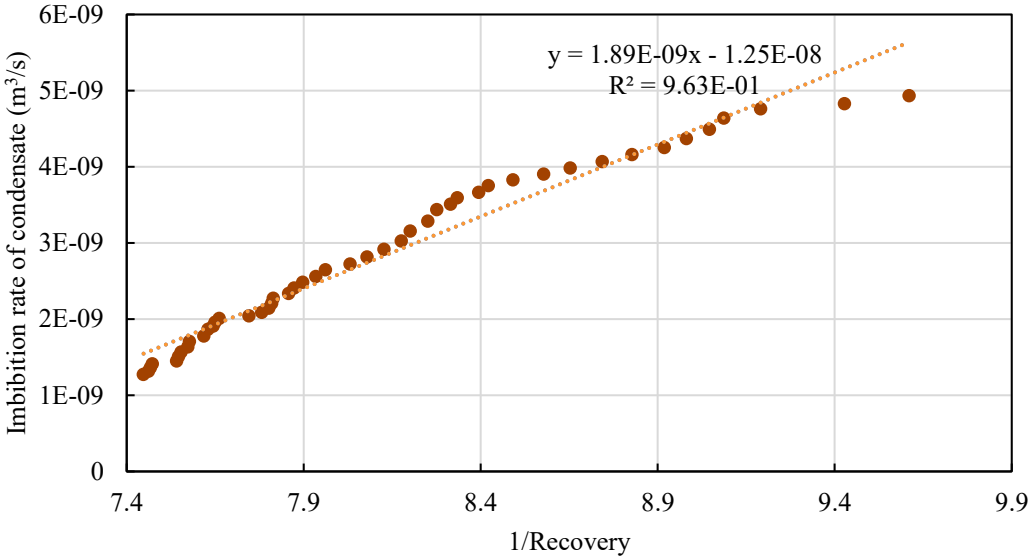



**Figure 34. Spontaneous imbibition rate of condensate versus the reciprocal of the gas recovery after wettability alteration.**

**Table 6. Liquid permeability and capillary pressure using spontaneous imbibition data after wettability alteration.**

| Liquid | k ($m^2$) | $P_c$ ($kg/m.s^2$) |
|---|---|---|
| Water | $7.96\times10^{-13}$ | $4.84\times10^{2}$ |
| Condensate | $8.28\times10^{-13}$ | $5.12\times10^{2}$ |

## 3.7. Spontaneous water imbibition under different initial water saturations

The presence of water is commonly observed in gas condensate reservoirs before liquid dropout. As a result, the recovery of gas through spontaneous water imbibition in core samples subjected to different $S_{wi}$ was examined. Spontaneous imbibition experiments were performed at four initial water saturations ($S_{wi}$) of 0, 11.46, 24.56, and 30%. The resulting gas recovery, reported in terms of pore volume (PV), is presented in Figure 35 for the natural

carbonate rock. It shows that the gas recovery (volume of imbibed liquid) in the units of PV increased with a decrease in $S_{wi}$.

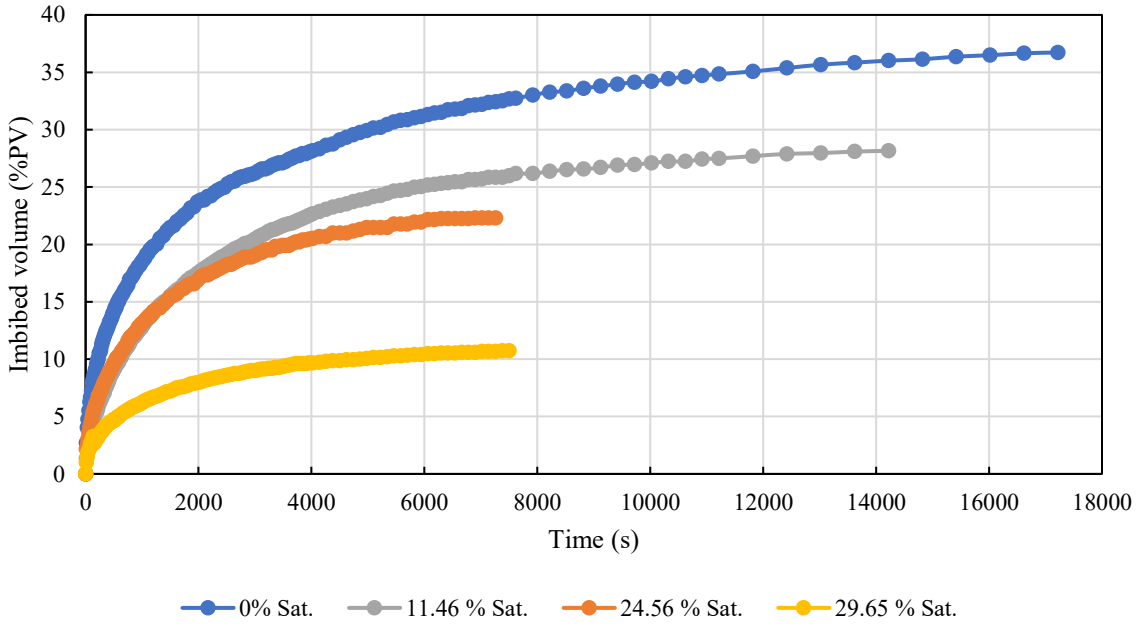



**Figure 35. Spontaneous water imbibition tests in different Swi of P1 core.**

Spontaneous imbibition is controlled by the interplay between capillary forces and viscous flow resistance [99-103]. As the initial water saturation increases, the capillary pressure gradient diminishes, leading to a lower driving force for liquid invasion. In contrast, a dry core ($S_{wi}$=0) offers fully accessible pore space, generating the largest capillary pressure gradient and, consequently, the most rapid initial imbibition. All pore sizes, from small to large, can be readily occupied by water. As the $S_{wi}$ increases, some of the smaller pores are already occupied by water, restricting subsequent imbibition to larger pores with lower capillary pressures. Therefore, the core with 11.46% $S_{wi}$ imbibes water more rapidly than that

with 24.56% $S_{wi}$, whereas the core with the highest initial water saturation (29.65%) exhibits the lowest cumulative imbibition volume.

As illustrated in Figure 36, increasing $S_{wi}$ consistently decreases the spontaneous imbibition rate (PV%/s) throughout the experiment, leading to a corresponding reduction in cumulative gas recovery.

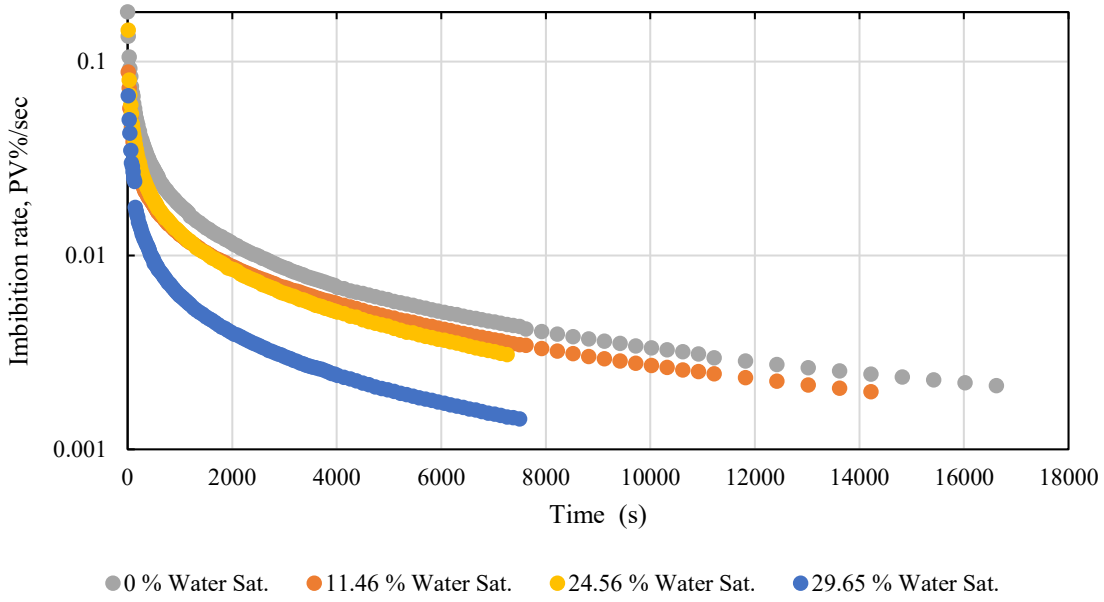



**Figure 36. Spontaneous water imbibition tests in different Swi of P1 core.**

## 3.8. Coreflooding

Generating data regarding two-phase flow is essential for predicting the result of wettability alteration for condensate banking prevention. Fluid flow in porous media is generally characterized by the superficial (Darcy) velocity, which is defined as the volumetric flow rate per unit bulk cross-sectional area of the rock. The corresponding expression for Darcy velocity is given in Eq. (18).

$$v = \frac{Q}{A} \tag{18}$$

where v denotes the Darcy velocity, Q represents the volumetric flow rate, and A is the bulk cross-sectional area of the core. In the pores of reservoir rocks, the flow velocity of a material point, $v_\phi$, is the real velocity, and the relationship between the real and Darcy velocity is written as Eq. (19).

$$v_\phi = \frac{v}{\phi} \tag{19}$$

where ϕ is the porosity of the core sample. In flow mechanics, the Reynolds number (Re) is an important physical quantity that judges the state of fluid flow. The Reynolds number in porous media is stated as Eq. (20).

$$\mathrm{Re} = \frac{v_\phi \sqrt{k}\rho}{1750\mu\phi^{\frac{3}{2}}} \tag{20}$$

where $v_\phi$ is the real flow velocity, cm/s; $k$ is the permeability, μm$^2$; $\rho$ is the density, g/cm$^3$; $\mu$ is the viscosity, mPa.s; and $\phi$ is the porosity. Darcy flow is in the laminar flow segment, where the Reynolds number is generally less than 0.2 or 0.3. The injection rates in all experiments mimic Darcy's velocity in the reservoir. The Reynolds number equivalent to 1 cc/min flow rate is $1.167\times10^{-6,}$ in which Re < 0.2, the flow is laminar flow, which satisfies Darcy's law. Eq. (21) and Eq. (22) were employed to calculate the residual fluid saturation and recovery factor, respectively.

$$\mathrm{Re}\,sidual\,Gas\,Saturation = \frac{V_{gi} - V_{gp}}{PV} \tag{21}$$

$$Gas\ \mathrm{Recovery} = \frac{V_{produced\ gas}}{PV} \quad \textbf{(22)}$$

### *3.8.1. Effect of injected liquid phase*

The surface tension of the injected liquid plays a key role in capillary trapping within a gas-saturated core by controlling the capillary entry pressure. A higher surface tension increases the pressure required for the liquid to invade smaller pores, thereby limiting its ability to displace the gas phase. Consequently, more gas remains trapped within the pore space, resulting in enhanced capillary trapping. It is obvious in Figure 37 that the pressure drop for water with higher surface tension is more than that of condensate. As reported in Table 7, at the BT time, the gas recovery during water injection was 27.60% while it was 62.37% when the injection phase was condensate. So, the recovered gas was more even at this time during condensate injection compared to water injection. Upon completion of the experiment, the trapped gas phase during water injection was 32.04%, and regarding the condensate injection, it was 24.55%. The endpoint relative permeability, the relative permeability of a fluid at the residual saturation of another immiscible fluid in the rock, for air/condensate is 2.65 times higher than that of air/water.

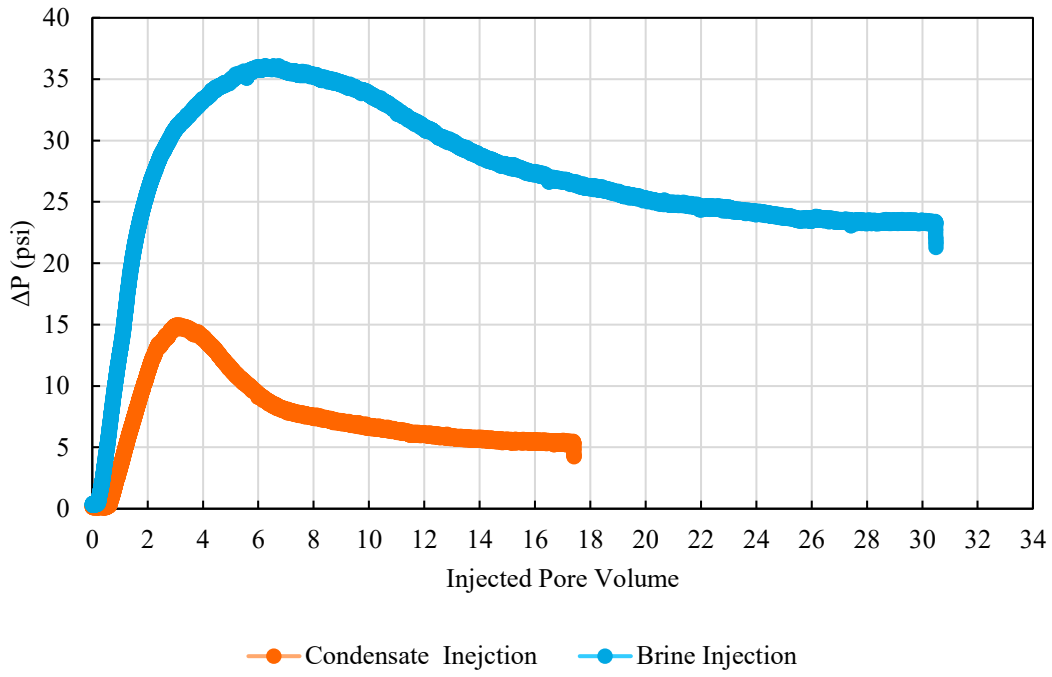



**Figure 37. Pressure drop during two different liquids versus injected pore volumes using an injection rate of 1 cc/min in P2.**

***Table 7. Core flooding results during different liquid injections at a constant 1 cc/min flow rate.***

| | BT time (min) | Gas recovery at BT time (%) | Trapped gas phase at the end of the experiment (cc) | Residual gas saturation (%) | End point relative permeability (mD) |
|---|---|---|---|---|---|
| Water | 21 | 27.60 | 5.05 | 32.04 | 6.3 |
| Condensate | 27 | 62.37 | 3.87 | 24.55 | 16.69 |

910

911 *3.8.2. Effect of flow rate*

The influence of injection rate on the forced imbibition process was evaluated by injecting liquid into an air-saturated, water-wet carbonate core at flow rates of 0.5, 1, and 2 cm³/min. As can be seen in Figure 38, by increasing the flow rate, the pressure drop vs injected PV increased.

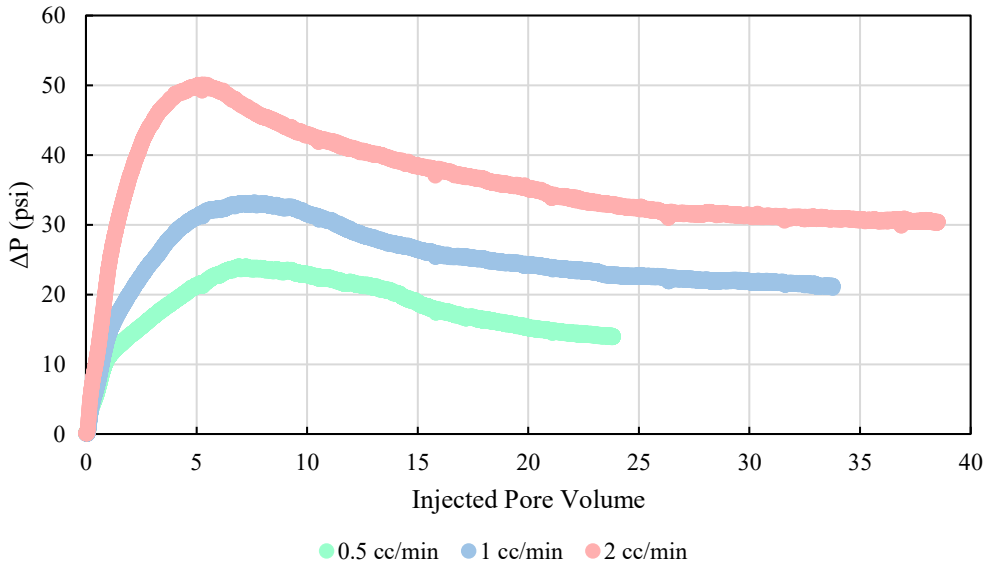



**Figure 38. Pressure drop during water injection as a function of injected pore volume for different flow rates of 0.5, 1, and 2 cm³/min during forced imbibition in untreated carbonate core P4.**

The results of the displacement process during these three flow rates are reported in Table 8.

**Table 8. Core flooding results during different flow rates of water injection into the air-saturated P4.**

| Fluid flow rate (cc/min) | BT time (min) | Gas recovery at BT time (%) | Trapped phase at the SS condition (cc) | Residual gas saturation (%) | Endpoint relative permeability (mD) |
|---|---|---|---|---|---|
| 0.5 | 26.17 | 59.23 | 5.92 | 37.54 | 5.17 |

| | | | | | |
|---|---|---|---|---|---|
| 1 | 14.29 | 61.32 | 3.01 | 19.09 | 6.89 |
| 2 | 8.30 | 63.66 | 1.88 | 11.92 | 9.54 |

A higher injection rate led to an earlier liquid breakthrough and resulted in a slight increase in gas production. The corresponding gas recoveries were 59.23%, 61.32%, and 63.66% at injection rates of 0.5, 1, and 2 $cm^3$/min, respectively. These results indicate relative increases in gas recovery of approximately 3.53% and 3.82% when the injection rate was doubled from 0.5 to 1 $cm^3$/min and from 1 to 2 $cm^3$/min, respectively. The increase in gas recovery became more pronounced at the end of the experiment, when the system reached steady-state (SS) conditions, with gas recovery increasing by approximately 41.02% as the injection rate was increased from 0.5 to 2 $cm^3$/min. The gas recoveries at BT and SS time for different flow rates before treatments are shown in Figure 39.

The endpoint relative permeabilities are also reported in Table 8. Increasing the injection rate from 0.5 to 2 $cm^3$/min increased the endpoint relative permeability by a factor of approximately 1.84, indicating a reduction in gas trapping.

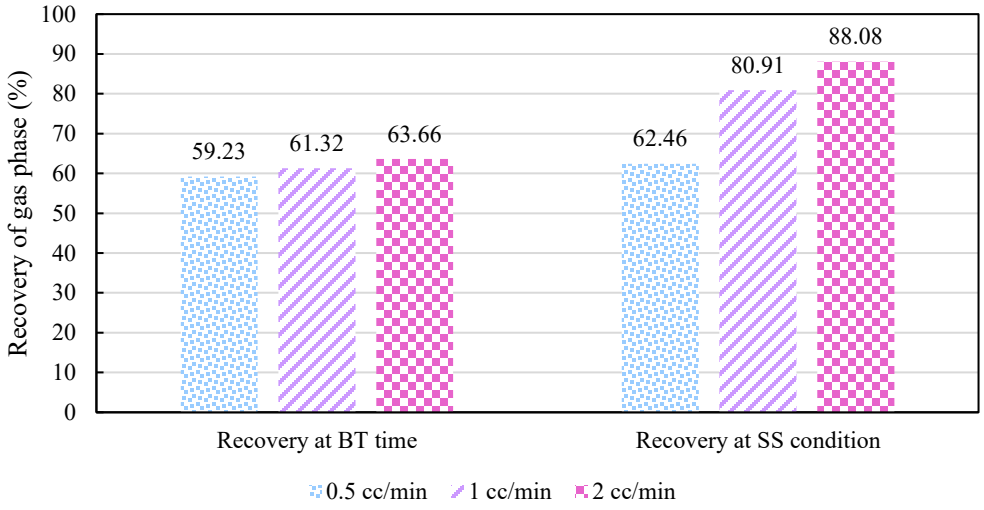
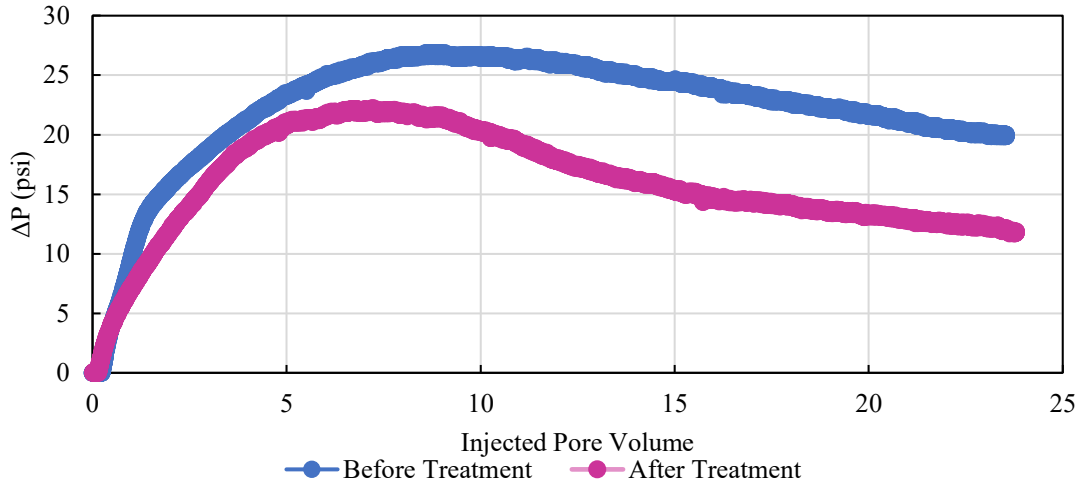



**Figure 39. Gas recovery at BT and SS time for different flow rates before treatments in P4.**

As reported in Table 8, the amount of trapped gas at a flow rate of 2 cc/min is 11.92. This value increases with decreasing flow rate. The effect of injection rate on the bypassing mechanism can be interpreted using the pore-doublet model. According to Chatzis and Dullien, higher displacement rates favor flow through larger pore channels, while the non-wetting phase becomes trapped in adjacent smaller pores, resulting in bypassing. Therefore, the amount of the trapped phase decreases. Furthermore, the snap-off mechanism is suppressed when the flow rate is high. A more detailed discussion of the underlying pore-scale mechanism is available in detail elsewhere [104, 105]. A similar trend was observed in the coreflooding experiments conducted in this study. Specifically, the endpoint liquid relative permeability, calculated from the final pressure drop, increased with increasing injection rate. These results indicate that, under the conditions investigated, higher injection rates reduced fluid trapping and improved recovery.

### *3.8.3. Effect of wettability*

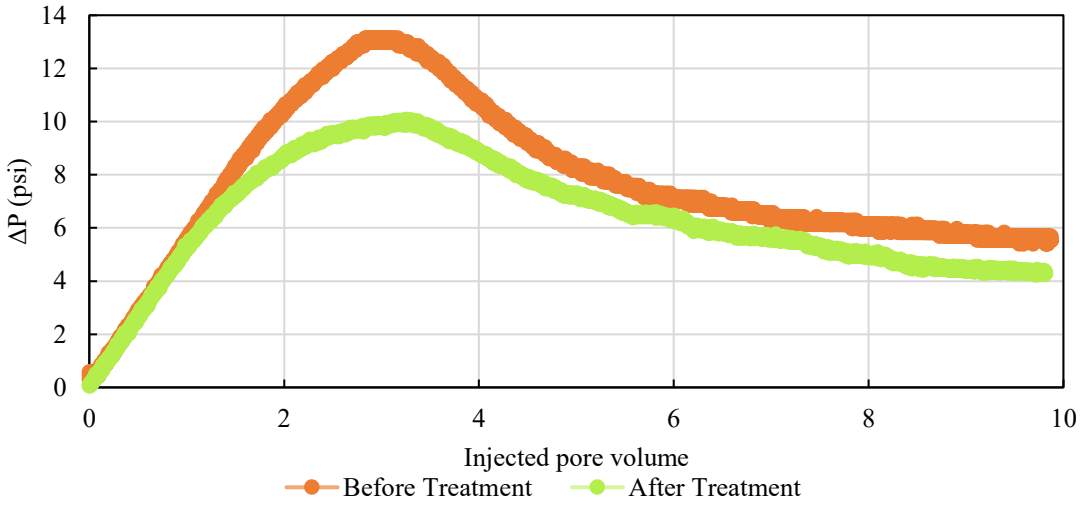
The wettability of the rock surface plays a significant role in the process of liquid injection into a gas-saturated core and can influence capillary trapping. If the rock surface is water-wet, the liquid phase tends to form a continuous film or bridge across the pore throats, making it difficult for the gas phase to flow and escape. This can result in increased capillary trapping of the gas phase. In contrast, if the rock is gas-wet, the liquid tends to form disconnected ganglia or droplets, allowing the gas phase to flow more easily and reducing capillary trapping. Before wettability alteration, injected water preferentially invaded smaller pores because of the strongly water-wet condition, resulting in higher capillary pressure and a larger pressure drop. After chemical treatment, the flow preferentially shifted toward larger pores with lower capillary pressure, leading to a 38.35% reduction in pressure drop and improved water mobility. A similar trend was observed during condensate injection, where the pressure drop decreased by 21.95% after treatment as condensate invaded larger pores. The pressure differences before and after wettability alteration for water and condensate are shown in Figure 40 and Figure 41. The endpoints' relative permeabilities of the water and condensate increased from 7.23 mD to 11.73 mD and from 14.59 mD to 18.69 mD, respectively, after WA.




963

964 **Figure 40. Pressure drop across carbonate core sample (P4) versus injected water pore volumes at 1**

965 **cc/min before and after treatment.**




966

967 **Figure 41. Pressure drop across carbonate core sample (P4) versus injected condensate pore volumes at**

968 **1 cc/min before and after treatment.**

969 In the performed coreflooding experiments, the core samples were initially dry and filled

970 with air, without undergoing prior vacuum saturation. Under these conditions, a portion of

971 the injected liquid is initially consumed in compressing and gradually displacing the trapped

air within the pore system before a continuous liquid pathway is formed. Consequently, the breakthrough occurred after more than 1 PV, which was also visually observed during the experiments. This delayed breakthrough primarily reflects the compressibility of the trapped gas phase and the capillary resistance opposing liquid entry into finer pores. Furthermore, the relatively low injection rates used enhance the dominance of capillary forces over viscous forces, leading to a gradual and stepwise advancement of the displacement front. Such behavior is typical for displacement tests on air-saturated cores without prior vacuum preparation and is consistent with the physical response of the system.

## 4. Conclusion

This study investigated wettability alteration as a strategy to reduce trapped fluids in carbonate rocks. Among the investigated chemicals, an anionic fluorosurfactant (FS) combined with hydrophobic $SiO_2$ nanoparticles exhibited the best performance. The optimal concentrations were 5 wt% FS and 0.5 wt% nanoparticles, increasing the water and condensate contact angles to 140.17° and 116.41°, respectively, while reducing the rock surface free energy from 68.64 to 1.72 mN/m. Capillary rise measurements further confirmed wettability alteration, with the water and condensate column heights decreasing from 24.60 to 4.48 mm and from 9.98 to 0 mm, respectively. Dynamic adsorption experiments demonstrated significant interaction between the surfactant and the carbonate surface, as confirmed by electrical conductivity measurements. Spontaneous imbibition tests showed successful wettability alteration, reducing water and condensate imbibition by 63.75% and

33.17%, respectively. Wettability alteration also reduced water permeability by 72.7% and increased the calculated capillary pressure by 23.5%, indicating the development of hydrophobic and oleophobic characteristics. In addition, lower initial water saturation promoted higher capillary pressure gradients and consequently higher imbibition rates. Coreflooding experiments demonstrated that the higher surface tension of water resulted in greater capillary trapping than condensate. At breakthrough, gas recovery reached 27.58% during water injection and 62.33% during condensate injection. At the end of the displacement, trapped gas saturation was 32.02% for water and 24.54% for condensate, while the endpoint relative permeability of the air–condensate system was 2.65 times that of the air–water system. Increasing the injection rate from 0.5 to 2 $cm^3$/min improved gas recovery by 41.02% and increased the endpoint relative permeability by 84.52%. Wettability alteration also reduced the pressure drop during fluid injection by 38.35% for water and 21.95% for condensate by shifting the preferential flow toward larger pores with lower capillary pressure. Consequently, the endpoint relative permeability increased from 7.23 to 11.73 mD for water and from 14.59 to 18.69 mD for condensate, corresponding to 1.62- and 1.28-fold increases, respectively. Overall, the results demonstrate that gas-wettability alteration effectively reduces capillary trapping, improves fluid mobility, and enhances displacement efficiency, highlighting its strong potential for improving gas condensate reservoir performance.

**List of Abbreviations**

| Abbreviations | Meaning |
|---|---|
| STB | Stock Tank Barrel |
| MMscf | Million Standard Cubic Feet |
| USA | United States of America |
| USBM | United States Bureau of Mines |
| FS | Fluoro Surfactant |
| CNT | Carbon Nano Tube |
| $TiO_2$ | Titanium Dioxide |
| MW | Molecular Weight |
| SFE | Surface Free Energy |
| NPs | Nano Particles |
| EGR | Enhanced Gas Recovery |
| WAG | Water Alternating Gas |
| WoS | Web of Science |
| VOS | Visualization of Similarities |
| IEA | International Energy Agency |
| $CO_2$ | Carbon Dioxide |
| $SiO_2$ | Silica |
| TCPFOS | Trichloro (perfluorooctyl) silane |
| IFT | Interfacial Tension |
| OWRK | Owens, Wendt, Rabel, and Kaelble |
| PV | Pore Volume |
| SI | Spontaneous Imbibition |
| EOR | Enhanced Oil Recovery |
| WA | Wettability Alteration |
| BWA | Before Wettability Alteration |
| AWA | After Wettability Alteration |
| CCA | Condensate Contact Angle |
| WCA | Water Contact Angle |

| Abbreviations | Meaning |
|---|---|
| EC | Electrical Conductivity |
| BT | Break Through |

1014

1015

## List of Nomenclature

| Nomenclature | Meaning |
|---|---|
| $h_l$ | liquid height |
| $\sigma$ | Surface tension |
| $\Delta\rho$ | Density difference |
| r | Capillary radius |
| $\gamma_{SL}$ | Interfacial tension between solid and liquid |
| $\gamma_{LG}$ | Surface tension between liquid and gas |
| $\gamma_{SG}$ | Interfacial tension between solid and gas |
| $\gamma_{SG}^{d}$ | Dispersion component of the SFE |
| $\gamma_{SG}^{P}$ | Polar component of the SFE |
| $\gamma_{SG}^{h}$ | Hydrogen-bonding component of the SFE |
| $\gamma_{SG}^{i}$ | Induction component of the SFE |
| $\gamma_{SG}^{ab}$ | Acid–base component of the SFE |
| $\theta$ | Contact angle |
| $S_{Li}$ | Initial liquid saturation |
| $W_{\text{after treatment}}$ | Weight of the core |
| $V_{\text{imb}}$ | Imbibed volume |
| $S_{\text{imb}}$ | Imbibed saturation |
| $Q_L$ | liquid imbibition rate |
| $N_{Lt}$ | Volume of liquid imbibed |
| $A$ | Cross-section area of the core |
| $\mu_L$ | Viscosity of liquid |
| $k_L$ | Effective permeability of liquid |
| $P_c$ | Capillary pressure |
| $S_{Lf}$, | Final water saturation |

| Nomenclature | Meaning |
|---|---|
| $S_{Li}$ | Initial water saturation |
| $L$ | Core length |
| g | Gravitational acceleration |
| $t$ | Imbibition time |
| $V_p$ | Pore volume |
| $\eta$ | Gas recovery achieved by water imbibition |
| $k$ | Permeability |

# 5. References


REFERENCES

[1] S. Alafnan, M. Aljawad, F. Alismail, and A. Almajed, "Enhanced Recovery from Gas Condensate Reservoirs through Renewable Energy Sources," *Energy & Fuels,* vol. 33, no. 10, pp. 10115-10122, 2019.

[2] J. Hagoort, *Fundamentals of gas reservoir engineering*. Elsevier, 1988.

[3] N. Miller, H. Nasrabadi, and D. Zhu, "Application of horizontal wells to reduce condensate blockage in gas condensate reservoirs," in *International Oil and Gas Conference and Exhibition in China*, 2010: OnePetro.

[4] B. Roussennac, "Gas condensate well test analysis," Stanford University, 2000.

[5] M. Qassamipour and A. Hashemi, "Mechanisms of liquid buildup in gas condensate reservoirs," *Petroleum science and technology,* vol. 29, no. 23, pp. 2425-2431, 2011.

[6] A. Arfanezhad and P. V. Valerievich, "Rapid Calculation of Well Productivity in Gas-condensate Reservoirs," 2022.

[7] Z. Wang *et al.*, "Experimental research of condensate blockage and mitigating effect of gas injection," *Petroleum,* vol. 4, no. 3, pp. 292-299, 2018.

[8] Q. Fevang and C. H. Whitson, "Modeling gas-condensate well deliverability," *SPE Reservoir Engineering,* vol. 11, no. 04, pp. 221-230, 1996.

[9] C. H. Whitson, Ø. Fevang, and T. Yang, "Gas condensate PVT–What's really important and Why?," in *IBC Conference, London, UK*, 1999, pp. 28-29.

[10] D. Marokane, A. Logmo-Ngog, and R. Sarkar, "Applicability of timely gas injection in gas condensate fields to improve well productivity," in *SPE/DOE Improved Oil Recovery Symposium*, 2002: Society of Petroleum Engineers.

[11] V. S. S. Bang *et al.*, "Improving productivity of hydraulically fractured gas condensate wells by chemical treatment," in *Offshore technology conference*, 2008: OnePetro.

[12] L. Fan *et al.*, "Understanding gas-condensate reservoirs," *Oilfield review,* vol. 17, no. 4, pp. 14-27, 2005.

[13] O. Fevang, "Gas condensate flow behavior and sampling," *October. University o f Trondheim,* 1995.

[14] S. Hinchman and R. Barree, "Productivity loss in gas condensate reservoirs," in *SPE Annual Technical Conference and Exhibition*, 1985: OnePetro.

[15] J.-R. Ursin, "Fluid flow in gas condensate reservoirs: the interplay of forces and their relative strengths," *Journal of Petroleum Science and Engineering,* vol. 41, no. 4, pp. 253-267, 2004.

[16] M. Magot, "Indigenous microbial communities in oil fields," *Petroleum microbiology,* pp. 21-33, 2005.

[17] A. Esmaeili, "Enhancing condensate recovery from gas condensate reservoirs through gas injection," 2015.

[18] J. Fahimpour, M. Jamiolahmady, R. Severac, and M. Sohrabi, "Performance of Fluorochemicals on Wettability Alteration of Carbonate Rocks to Alleviate Condensate/Water Banking," in *Paper SCA presented at the International Symposium of the Society of Core Analysts*, 2012, pp. 27-30.

[19] M. Cimolai, R. Gies, D. Bennion, and D. Myers, "Mitigating horizontal well formation damage in a low-permeability conglomerate gas reservoir," in *SPE Gas Technology Symposium*, 1993: Society of Petroleum Engineers.

[20] A. H. El-Banbi, W. McCain Jr, and M. Semmelbeck, "Investigation of well productivity in gas-condensate reservoirs," in *SPE/CERI Gas Technology Symposium*, 2000: Society of Petroleum Engineers.

[21] R. Engineer, "Cal Canal field, California: Case history of a tight and abnormally pressured gas condensate reservoir," in *SPE California Regional Meeting*, 1985: Society of Petroleum Engineers.

[22] J. W. Ely, B. C. Wolters, and W. D. McCain, "Method for reducing permeability restriction near wellbore," ed: Google Patents, 2005.

[23] V. Bang, *Development of a successful chemical treatment for gas wells with condensate or water blocking damage*. The University of Texas at Austin, 2007.

[24] W. Assiri and J. L. Miskimins, "The water blockage effect on desiccated tight gas reservoir," in *SPE International Symposium and Exhibition on Formation Damage Control*, 2014: OnePetro.

[25] A. A. Roozshenas, H. Hematpur, R. Abdollahi, and H. Esfandyari, "Water production problem in gas reservoirs: concepts, challenges, and practical solutions," *Mathematical Problems in Engineering,* vol. 2021, 2021.

[26] T. Geffen, D. Parrish, G. Haynes, and R. Morse, "Efficiency of gas displacement from porous media by liquid flooding," *Journal of Petroleum Technology,* vol. 4, no. 02, pp. 29-38, 1952.

[27] N. Van Eck and L. Waltman, "Software survey: VOSviewer, a computer program for bibliometric mapping," *scientometrics,* vol. 84, no. 2, pp. 523-538, 2010.

[28] N. J. Van Eck and L. Waltman, "Text mining and visualization using VOSviewer," *arXiv preprint arXiv:1109.2058,* 2011.

[29] M. A. Sayed and G. A. Al-Muntasheri, "Mitigation of the effects of condensate banking: a critical review," *SPE production & Operations,* vol. 31, no. 02, pp. 85-102, 2016.

[30] F. Kazemi *et al.*, "Wettability alteration in gas condensate reservoirs: A critical review of the opportunities and challenges," *Energy & Fuels,* vol. 38, no. 3, pp. 1539-1565, 2024.

[31] K. Li and A. Firoozabadi, "Experimental study of wettability alteration to preferential gas-wetting in porous media and its effects," *SPE Reservoir Evaluation & Engineering,* vol. 3, no. 02, pp. 139-149, 2000.

[32] M. Sheydaeemehr, B. Sedaeesola, and A. Vatani, "Gas-condensate production improvement using wettability alteration: a giant gas condensate field case study," *Journal of Natural Gas Science and Engineering,* vol. 21, pp. 201-208, 2014.

[33] V. S. S. Bang, G. A. Pope, M. M. Sharma, J. R. Baran Jr, and M. Ahmadi, "A new solution to restore productivity of gas wells with condensate and water blocks," in *SPE Annual Technical Conference and Exhibition*, 2008: Society of Petroleum Engineers.

[34] S. Wu and A. Firoozabadi, "Permanent alteration of porous media wettability from liquid-wetting to intermediate gas-wetting," *Transport in Porous Media,* vol. 85, no. 1, pp. 189-213, 2010.

[35] N. Salmani, R. Fatehi, and R. Azin, "On the liquid condensate vertical migration near the production wells of gas-condensate reservoirs," *Engineering Science and Technology, an International Journal,* vol. 23, no. 4, pp. 715-722, 2020.

[36] M. M. Fahes and A. Firoozabadi, "Wettability alteration to intermediate gas-wetting in gas-condensate reservoirs at high temperatures," *SPE Journal,* vol. 12, no. 04, pp. 397-407, 2007.

[37] E. Kissa, *Fluorinated surfactants and repellents*. CRC Press, 2001.

[38] G.-Q. Tang and A. Firoozabadi, "Relative permeability modification in gas-liquid systems through wettability alteration to intermediate gas-wetting," in *SPE Annual Technical Conference and Exhibition*, 2000: Society of Petroleum Engineers.

[39] G.-Q. Tang and A. Firoozabadi, "Wettability alteration to intermediate gas-wetting in porous media at elevated temperatures," *Transport in Porous Media,* vol. 52, no. 2, pp. 185-211, 2003.

[40] B. Adibhatla, K. Mohanty, P. Berger, and C. Lee, "Effect of surfactants on wettability of near-wellbore regions of gas reservoirs," *Journal of petroleum science and engineering,* vol. 52, no. 1-4, pp. 227-236, 2006.

[41] M. Noh and A. Firoozabadi, "Effect of wettability on high-velocity coefficient in two-phase gas/liquid flow," *SPE Journal,* vol. 13, no. 03, pp. 298-304, 2008.

[42] R.-S. Rocke, M. Sharma, V. Bang, M. Ahmadi, and H. Linnemeyer, "Improving well productivity in gas condensate reservoirs via chemical treatment," in *Tobago gas technology conference. The University of Trindad and Tobago, Lowlands, Tobago*, 2008.

[43] V. Bang, G. A. Pope, M. M. Sharma, J. R. Baran, and M. Ahmadi, "A new solution to restore productivity of gas wells with condensate and water blocks," *SPE Reservoir Evaluation & Engineering,* vol. 13, no. 02, pp. 323-331, 2010.

[44] M. Ahmadi, M. M. Sharma, G. Pope, D. E. Torres, C. A. McCulley, and H. Linnemeyer, "Chemical treatment to mitigate condensate and water blocking in gas wells in carbonate reservoirs," *SPE Production & Operations,* vol. 26, no. 01, pp. 67-74, 2011.

[45] K. Li, Y. Liu, H. Zheng, G. Huang, and G. Li, "Enhanced gas-condensate production by wettability alteration to gas wetness," *Journal of Petroleum Science and Engineering,* vol. 78, no. 2, pp. 505-509, 2011.

[46] A. Karimi *et al.*, "Wettability alteration in carbonates using zirconium oxide nanofluids: EOR implications," *Energy & Fuels,* vol. 26, no. 2, pp. 1028-1036, 2012.

[47] C. Franco, O. Botero, J. Zapata, E. Mora, C. Candela, and A. Castillo, "Inhibited gas stimulation to mitigate condensate banking and maximize recovery in cupiagua field," *SPE production & operations,* vol. 28, no. 02, pp. 154-167, 2013.

[48] G. Jiang, Y. Li, and M. Zhang, "Evaluation of gas wettability and its effects on fluid distribution and fluid flow in porous media," *Petroleum Science,* vol. 10, pp. 515-527, 2013.

[49] M. Mousavi, S. Hassanajili, and M. Rahimpour, "Synthesis of fluorinated nano-silica and its application in wettability alteration near-wellbore region in gas condensate reservoirs," *Applied Surface Science,* vol. 273, pp. 205-214, 2013.

[50] S. Sharifzadeh, S. Hassanajili, and M. Rahimpour, "Wettability alteration of gas condensate reservoir rocks to gas wetness by sol–gel process using fluoroalkylsilane," *Journal of Applied Polymer Science,* vol. 128, no. 6, pp. 4077-4085, 2013.

[51] J. Fahimpour and M. Jamiolahmady, "Impact of gas-condensate composition and interfacial tension on oil-repellency strength of wettability modifiers," *Energy & fuels,* vol. 28, no. 11, pp. 6714-6722, 2014.

[52] S. Zhang *et al.*, "Wettability alteration to intermediate gas-wetting in low-permeability gas-condensate reservoirs," *Journal of Petroleum Exploration and Production Technology,* vol. 4, pp. 301-308, 2014.

[53] J. Fahimpour and M. Jamiolahmady, "Optimization of fluorinated wettability modifiers for gas/condensate carbonate reservoirs," *SPE Journal,* vol. 20, no. 04, pp. 729-742, 2015.

[54] G. Karandish, M. Rahimpour, S. Sharifzadeh, and A. Dadkhah, "Wettability alteration in gas-condensate carbonate reservoir using anionic fluorinated treatment," *Chemical Engineering Research and Design,* vol. 93, pp. 554-564, 2015.

[55] S. Sharifzadeh, S. Hassanajili, M. Rahimpour, and M. Mousavi, "Preparation of the modified limestone possessing higher permeability of gas well based on fluorinated silica: Effect of catalyst," *Journal of Fluorine Chemistry,* vol. 173, pp. 35-46, 2015.

[56] P. Esmaeilzadeh, M. T. Sadeghi, Z. Fakhroueian, A. Bahramian, and R. Norouzbeigi, "Wettability alteration of carbonate rocks from liquid-wetting to ultra gas-wetting using TiO2, SiO2 and CNT nanofluids containing fluorochemicals, for enhanced gas recovery," *Journal of Natural Gas Science and Engineering,* vol. 26, pp. 1294-1305, 2015.

[57] M. Aminnaji, H. Fazeli, A. Bahramian, S. Gerami, and H. Ghojavand, "Wettability alteration of reservoir rocks from liquid wetting to gas wetting using nanofluid," *Transport in Porous Media,* vol. 109, no. 1, pp. 201-216, 2015.

[58] J. Jin, Y. Wang, K. Wang, J. Ren, B. Bai, and C. Dai, "The effect of fluorosurfactant-modified nano-silica on the gas-wetting alteration of sandstone in a CH4-liquid-core system," *Fuel,* vol. 178, pp. 163-171, 2016.

[59] R. Saboori, R. Azin, S. Osfouri, S. Sabbaghi, and A. Bahramian, "Synthesis of fluorine-doped silica-coating by fluorosilane nanofluid to ultrahydrophobic and ultraoleophobic surface," *Materials Research Express,* vol. 4, no. 10, p. 105010, 2017.

[60] M. Sayed, F. Liang, and H. Ow, "Novel surface modified nanoparticles for mitigation of condensate and water blockage in gas reservoirs," in *SPE International Conference and Exhibition on Formation Damage Control*, 2018: Society of Petroleum Engineers.

[61] I. Nowrouzi, A. Khaksar Manshad, and A. H. Mohammadi, "Wettability alteration and enhanced gas condensate recovery by treatment of carbonate reservoir rock using supercritical R134A and R404A

gases," *Journal of Petroleum Exploration and Production Technology,* vol. 10, no. 8, pp. 3751-3766, 2020a.

[62] M. A. Tabar, Y. Shafiei, M. Shayesteh, A. D. Monfared, and M. H. Ghazanfari, "Wettability alteration of calcite rock from gas-repellent to gas-wet using a fluorinated nanofluid: a surface analysis study," *Journal of Natural Gas Science and Engineering,* vol. 83, p. 103613, 2020.

[63] M. Shayesteh, M. A. Tabar, Y. Shafiei, Z. Fakhroueian, and M. H. Ghazanfari, "On the adsorption behavior of a fluorochemical onto carbonate rock with the application of wettability alteration to a gas wetting condition," *Journal of Molecular Liquids,* vol. 326, p. 115031, 2021.

[64] I. Nowrouzi, A. H. Mohammadi, and A. Khaksar Manshad, "Modifying the Wettability of Carbonate Gas Condensate Reservoirs Rocks toward Gasophilic for Condensate Blockage Removal and Enhanced Hydrocarbon Recovery Using a Synthesized Anionic Fluorinated Surfactant," *Energy & Fuels,* vol. 37, no. 16, pp. 11707-11719, 2023.

[65] F. Kazemi, R. Azin, and S. Osfouri, "Gas condensate recovery in carbonate rocks through wettability alteration: Characterization and Optimization by Response Surface Methodology (RSM)," *Petroleum,* 2026.

[66] R. Nazari Moghaddam, A. Bahramian, Z. Fakhroueian, A. Karimi, and S. Arya, "Comparative study of using nanoparticles for enhanced oil recovery: wettability alteration of carbonate rocks," *Energy & Fuels,* vol. 29, no. 4, pp. 2111-2119, 2015.

[67] E. W. Washburn, "The dynamics of capillary flow," *Physical review,* vol. 17, no. 3, p. 273, 1921.

[68] B. Yang and Q. Chang, "Wettability studies of filter media using capillary rise test," *Separation and Purification Technology,* vol. 60, no. 3, pp. 335-340, 2008.

[69] A. Siebold, A. Walliser, M. Nardin, M. Oppliger, and J. Schultz, "Capillary rise for thermodynamic characterization of solid particle surface," *Journal of colloid and interface science,* vol. 186, no. 1, pp. 60-70, 1997.

[70] L. Galet, S. Patry, and J. Dodds, "Determination of the wettability of powders by the Washburn capillary rise method with bed preparation by a centrifugal packing technique," *Journal of colloid and interface science,* vol. 346, no. 2, pp. 470-475, 2010.

[71] J. Jin *et al.*, "Gas-wetting alteration by fluorochemicals and its application for enhancing gas recovery in gas-condensate reservoirs: a review," *Energies,* vol. 13, no. 18, p. 4591, 2020.

[72] J. Jin, Y. Wang, T. A. Nguyen, A. V. Nguyen, M. Wei, and B. Bai, "The effect of gas-wetting nano-particle on the fluid flowing behavior in porous media," *Fuel,* vol. 196, pp. 431-441, 2017.

[73] F. Fang, A. Firoozabadi, M. Abbaszadeh, and C. Radke, "A Phenomenological modeling of critical condensate saturation," in *SPE Annual Technical Conference and Exhibition?*, 1996, pp. SPE-36716-MS: SPE.

[74] F. Hejda, P. Solar, and J. Kousal, "Surface free energy determination by contact angle measurementsΓÇôa comparison of various approaches," in *WDS*, 2010, vol. 10, pp. 25-30.

[75] F. M. Fowkes, "Attractive forces at interfaces," *Industrial & Engineering Chemistry,* vol. 56, no. 12, pp. 40-52, 1964.

[76] D. Kaelble, "Dispersion-polar surface tension properties of organic solids," *The Journal of Adhesion,* vol. 2, no. 2, pp. 66-81, 1970.

[77] D. K. Owens and R. Wendt, "Estimation of the surface free energy of polymers," *Journal of applied polymer science,* vol. 13, no. 8, pp. 1741-1747, 1969.

[78] W. Rabel, "Einige Aspekte der Benetzungstheorie und ihre Anwendung auf die Untersuchung und Ver├ñnderung der Oberfl├ñcheneigenschaften von Polymeren," *Farbe und Lack,* vol. 77, no. 10, pp. 997-1005, 1971.

[79] Y. Wang, Y. Li, Q. Wang, Q. Li, Y. Zhang, and L. Yuan, "Synthesis and evaluation of properties of N, N-bis (perfluorooctyl) imine acetate sodium as a gas-wetting alteration agent," *RSC advances,* vol. 8, no. 15, pp. 7924-7931, 2018.

[80] K. Hashizaki *et al.*, "A Method for Measuring the Surface Free Energy of Topical Semi-solid Dosage Forms," *Chemical and Pharmaceutical Bulletin,* vol. 69, no. 11, pp. 1083-1087, 2021.

[81] S. Wu and A. Firoozabadi, "Effect of salinity on wettability alteration of porous media from liquid wetting to intermediate gas wetting," in *SPE International Symposium on Oilfield Chemistry*, 2009: OnePetro.

[82] A. M. Moghadam and M. B. Salehi, "Enhancing hydrocarbon productivity via wettability alteration: a review on the application of nanoparticles," *Reviews in Chemical Engineering,* vol. 35, no. 4, pp. 531-563, 2019.

[83] H. R. E. Gahrooei and M. H. Ghazanfari, "Toward a hydrocarbon-based chemical for wettability alteration of reservoir rocks to gas wetting condition: Implications to gas condensate reservoirs," *Journal of Molecular Liquids,* vol. 248, pp. 100-111, 2017.

[84] L. Kewen and F. Abbas, "Experimental study of wettability alteration to preferential gas-wetting in porous media and its effects," *SPE Reservoir Evaluation & Engineering,* vol. 3, no. 02, pp. 139-149, 2000.

[85] B. Hou, R. Jia, M. Fu, L. Li, T. Xu, and C. Jiang, "Mechanism of synergistically changing wettability of an oil-wet sandstone surface by a novel nanoactive fluid," *Energy & Fuels,* vol. 34, no. 6, pp. 6871-6878, 2020.

[86] X. Xie, Y. Liu, M. M. Sharma, and W. W. Weiss, "Wettability alteration to increase deliverability of gas production wells," in *SPE Eastern Regional/AAPG Eastern Section Joint Meeting*, 2008: OnePetro.

[87] K. Li and R. N. Horne, "Characterization of spontaneous water imbibition into gas-saturated rocks," in *SPE Western Regional Meeting*, 2000, pp. SPE-62552-MS: SPE.

[88] D. Y. Kwok and A. W. Neumann, "Contact angle measurement and contact angle interpretation," *Advances in colloid and interface science,* vol. 81, no. 3, pp. 167-249, 1999.

[89] M. Palencia, "Surface free energy of solids by contact angle measurements," *J. Sci. Technol. Appl,* vol. 2, p. 84, 2017.

[90] I. Jordanov and B. Mangovska, "Characterization on surface of mercerized and enzymatic scoured cotton after different temperature of drying," *The Open Textile Journal,* vol. 2, no. 1, 2009.

[91] Y. Sokolova, A. Ayzenshtadt, and V. Strokova, "Evaluation of dispersion interaction in glyoxal/silica organomineral system," in *Journal of Physics: Conference Series*, 2017, vol. 929, no. 1, p. 012110: IOP Publishing.

[92] Y. Wang, J. Jin, L. Ma, L. Li, and X. Zhao, "Influence of wettability alteration to preferential gas-wetting on displacement efficiency at elevated temperatures," *Journal of dispersion science and technology,* vol. 36, no. 9, pp. 1274-1281, 2015.

[93] Y. Li, Y. Wang, G. Guo, K. Wang, F. Gomado, and C. Zhang, "The effect of fluorocarbon surfactant on the gas-wetting alteration of reservoir," *Petroleum Science and Technology,* vol. 36, no. 13, pp. 951-958, 2018.

[94] H. E. Gahrooei, E. Joonaki, M. H. Ghazanfari, S. Ghanaatian, and A. H. Youzband, "Introduction of a new hydrocarbon based chemical for wettability alteration of reservoir rocks to gas wetting condition," in *79th EAGE Conference and Exhibition 2017*, 2017, vol. 2017, no. 1, pp. 1-5: European Association of Geoscientists & Engineers.

[95] S. Zhang *et al.*, "Wettability alteration to intermediate gas-wetting in low-permeability gas-condensate reservoirs," *Journal of Petroleum Exploration and Production Technology,* vol. 4, no. 3, pp. 301-308, 2014.

[96] H. R. E. Gahrooei and M. H. Ghazanfari, "Application of a water based nanofluid for wettability alteration of sandstone reservoir rocks to preferentially gas wetting condition," *Journal of Molecular Liquids,* vol. 232, pp. 351-360, 2017.

[97] A. Safaei, F. Esmaeilzadeh, A. Sardarian, S. M. Mousavi, and X. Wang, "Experimental investigation of wettability alteration of carbonate gas-condensate reservoirs from oil-wetting to gas-wetting using Fe3O4 nanoparticles coated with Poly (vinyl alcohol),(PVA) or Hydroxyapatite (HAp)," *Journal of Petroleum Science and Engineering,* vol. 184, p. 106530, 2020.

[98] M. Franco-Aguirre, R. D. Zabala, S. H. Lopera, C. A. Franco, and F. B. Cortés, "Interaction of anionic surfactant-nanoparticles for gas-Wettability alteration of sandstone in tight gas-condensate reservoirs," *Journal of Natural Gas Science and Engineering,* vol. 51, pp. 53-64, 2018.

[99] K. Li, K. Chow, and R. N. Horne, "Influence of initial water saturation on recovery by spontaneous imbibition in gas/water/rock systems and the calculation of relative permeability," *SPE Reservoir Evaluation & Engineering,* vol. 9, no. 04, pp. 295-301, 2006.

[100] B. Viksund, N. Morrow, S. Ma, W. Wang, and A. Graue, "Initial water saturation and oil recovery from chalk and sandstone by spontaneous imbibition," in *Proceedings, 1998 International Symposium of Society of Core Analysts, The Hague*, 1998.

[101] S. Akin, J. Schembre, S. Bhat, and A. Kovscek, "Spontaneous imbibition characteristics of diatomite," *Journal of Petroleum Science and Engineering,* vol. 25, no. 3-4, pp. 149-165, 2000.

[102] J. Cai, B. Yu, M. Zou, and L. Luo, "Fractal characterization of spontaneous co-current imbibition in porous media," *Energy & Fuels,* vol. 24, no. 3, pp. 1860-1867, 2010.

[103] L. Handy, "Determination of effective capillary pressures for porous media from imbibition data," *Transactions of the AIME,* vol. 219, no. 01, pp. 75-80, 1960.

[104] I. Chatzis and F. Dullien, "Dynamic immiscible displacement mechanisms in pore doublets: theory versus experiment," *Journal of Colloid and Interface Science,* vol. 91, no. 1, pp. 199-222, 1983.

[105] F. Kazemi, R. Azin, and S. Osfouri, "Evaluation of phase trapping models in gas-condensate systems in an unconsolidated sand pack," *Journal of Petroleum Science and Engineering,* vol. 195, p. 107848, 2020.